eLife

Reviewed Preprint
v1 • December 19, 2024
Not revised

Reviewed Preprint
v2 • May 12, 2026
Revised by authors

Dorsal/NF-κB exhibits a dorsal-to-ventral mobility gradient in the Drosophila embryo

Hadel Al Asafen[a,*], Natalie M Clark[b,*], Etika Goyal[a,*], Sadia Siddika Dima[a], Hung-Yuan Chen[a], Thomas Jacobsen[c], Rosangela Sozzani[b], Gregory T Reeves[a,d]

[a]Artie McFerrin Department of Chemical Engineering, Texas A&M University, College Station, United States • [b]Department of Plant and Microbial Biology, North Carolina State University, Raleigh, United States • [c]Department of Chemical and Biomolecular Engineering, North Carolina State University, Raleigh, United States • [d]Interdisciplinary Graduate Program in Genetics and Genomics, Texas A&M University, College Station, United States

For correspondence: gtreeves@tamu.edu

* These authors contributed equally to this work

Competing interests: No competing interests declared

Funding: See page 18

Reviewing editor: Marcos Nahmad, Center for Research and Advanced Studies of the National Polytechnic Institute, Mexico

eLife Assessment

This **valuable** study provides quantitative data and analysis to reveal that variations in Dorsal (Dl) nuclear dynamics along the Dorso-ventral axis in the early Drosophila embryo are governed by Dl-Cactus nuclear interactions. The **solid** evidence partially supports a mechanism where nuclear localized Cactus contributes to the fraction of Dl that binds to DNA, but additional work will be necessary to confirm the claims and the biological significance of these findings.

https://doi.org/10.7554/eLife.100462.2.sa3

Abstract

Morphogen-mediated patterning is a highly dynamic developmental process. To obtain an accurate understanding of morphogen gradient formation and downstream gene expression, biophysical parameters such as protein mobilities must be quantified *in vivo*. The dorsal-ventral (DV) patterning of early *Drosophila* embryos by the NF-κB homolog Dorsal (Dl) is an excellent system for understanding morphogen gradient formation. Dl gradient formation is controlled by the inhibitor Cactus/IκB (Cact), which regulates the nuclear import and diffusion of Dl protein. However, quantitative measurements of Dl mobility and binding are currently lacking. Here, we use scanning fluorescence correlation spectroscopy to quantify the mobility of GFP-tagged Dl. We find that the DNA binding of Dl-GFP, which affects its mobility, varies along the DV axis, with highest DNA binding on the ventral side. Moreover, we also observe that the time scale for Dl-GFP to exit the nucleus is longer in the ventral and lateral regions of the embryo, which is consistent with stronger DNA binding. Using analysis of mutant alleles of *dl* tagged with GFP, we conclude that Dl-GFP/Cact interactions in the nuclei are responsible for the variation in Dl-GFP/DNA binding along the DV axis, which impacts our understanding of the spatial range of the Dl gradient and the robustness and precision of downstream gene expression. Thus, our results highlight the complexity of morphogen gradient dynamics and the ability of quantitative measurements of biophysical interactions to drive biological discovery.

Introduction

Tissues in a developing organism are patterned by short and long-range signaling achieved through morphogen concentration gradients, which carry the positional information necessary to control gene expression in a spatially dependent fashion. In the past two decades, studies using GFP-tagged morphogens -- including early *Drosophila* morphogens Bicoid and Dorsal; Dpp in the wing imaginal disc; and the Hedgehog, Wnt, and TGF-β families in vertebrates -- have revealed that the establishment of morphogen gradients is a highly dynamic and complex process (Delotto

et al., 2007; Entchev et al., 2000; Gregor et al., 2007; Holzer et al., 2012; Luz et al., 2014; Reeves et al., 2012; Ribes et al., 2010; Teleman & Cohen, 2000; Wallkamm et al., 2014; Wartlick et al., 2011; Williams et al., 2004; Zhou et al., 2012). To move toward a quantitative understanding of morphogen signaling and downstream gene expression patterns, several key biophysical parameters related to gradient formation, including diffusivity and binding, must be measured.

Dorsal (Dl), one of three *Drosophila* orthologs to mammalian NF-κB (Steward, 1987), acts as a morphogen to pattern the dorsal-ventral (DV) axis of blastoderm stage (1-3 h old) *Drosophila* embryos. Dl is initially distributed uniformly along the DV axis (Roth et al., 1989; Steward et al., 1988). After the 9th nuclear division cycle, when the nuclei migrate to the periphery of the syncytial embryo, Dl begins to accumulate in ventral nuclei, and is excluded from dorsal nuclei (Roth et al., 1989; Steward et al., 1988). This DV gradient in Dl nuclear concentration is due to signaling through the Toll receptor on the ventral side of the embryo (Anderson, Bokla, et al., 1985; Anderson, Jürgens, et al., 1985; Belvin & Anderson, 1996). In the absence of Toll signaling, Dl remains bound by the cytoplasmic tethering protein Cactus (Cact), the *Drosophila* IκB homolog (Geisler et al., 1992; Kidd, 1992), and thus localized to the cytoplasm (Belvin et al., 1995; Bergmann et al., 1996; Reach et al., 1996; Whalen & Steward, 1993). On the ventral side, Toll signaling acts through Pelle kinase to phosphorylate Cact, which causes dissociation of the Dl/Cact complex and degradation of Cact (Daigneault et al., 2013). Once freed from binding to Cact, Dl enters the nucleus and regulates the expression of more than 50 target genes, which initiate further signaling pathways and specification of the embryo's germ layers (Chopra & Levine, 2009; Moussian & Roth, 2005; Reeves & Stathopoulos, 2009; Schloop, Bandodkar, et al., 2020; Stathopoulos & Levine, 2002, 2004). Toll signaling also phosphorylates Dl, which has been shown to increase Dl nuclear localization (Drier et al., 1999, 2000; Gillespie & Wasserman, 1994; Whalen & Steward, 1993).

While this well-established mechanism rapidly initiates Dl gradient formation, recent work has revealed complex dynamics in the further maturation of the gradient. In particular, live imaging of fluorescently-tagged Dl proteins has shown that the Dl nuclear gradient grows slowly during interphase and collapses during mitosis (Delotto et al., 2007; Reeves et al., 2012). Quantification of the gradient levels has shown that over the course of nuclear cycle 10-14, Dl (both nuclear and cytoplasmic) accumulates on the ventral side of the embryo, causing the peak of the Dl gradient, in the ventral-most cells, to grow steadily over time (Carrell et al., 2017; Liberman et al., 2009; O'Connell & Reeves, 2015; Reeves et al., 2012; Schloop, Carrell-Noel, et al., 2020). In particular, diffusion and nuclear capture of Dl, both of which are regulated by Cact, are proposed to control the continuous growth of the Dl gradient peak (Carrell et al., 2017). Nonetheless, the diffusivity and nuclear transport rates are not quantitatively known. Furthermore, our previous work has suggested that Dl/Cact complex also is present in the nucleus, which has implications for the apparent spatial range of the Dl gradient, as well as for the robustness and precision of gene expression (Al Asafen et al., 2020; O'Connell & Reeves, 2015). Therefore, to fully understand the dynamics of Dl gradient formation and gene regulation, measurements of the biophysical parameters governing Dl mobility (specifically diffusivity, nuclear transport, and binding to DNA) are needed.

Here we employ scanning fluorescence correlation spectroscopy (scanning FCS) techniques to measure the mobility of Dl in live embryos. Scanning FCS techniques involve rapid and repeated acquisition of fluorescent imaging data using confocal microscopy. First, we apply a specific scanning FCS method known as Raster Image Correlation Spectroscopy (RICS) to autocorrelate GFP-tagged Dl over space and time in a small region of the embryo (Digman, Brown, et al., 2005; Digman, Sengupta, et al., 2005). The shape of this autocorrelation function is then analyzed to infer protein diffusion, which reveals two pools of Dl-GFP, mobile and immobile. Notably, we observed that the fraction of immobile Dl varies along the DV axis. Cross-correlation RICS (ccRICS), which uses two different fluorophores (GFP and RFP, in this case), suggests that the DV variation in immobile fraction is the result of a higher fraction of Dl binding to the DNA on the ventral side than on the dorsal side. In addition, we employ Pair Correlation Function (pCF) technique to

compute the correlation between two pixels along a line scan, allowing us to visualize barriers to Dl movement (Digman & Gratton, 2009; Hinde et al., 2010). We show that the tendency of a Dl-GFP molecule to exit the nucleus also displays variation along the DV axis. When examining mutants that mimic the Dl gradient at different DV positions, the RICS and pCF data corroborate these findings. We propose two competing hypotheses to explain the DV variation in Dl/DNA interactions: that Toll phosphorylation of Dl may increase Dl/DNA interactions on the ventral side, or that Cact may bind Dl in the nuclei, which would prevent Dl from binding DNA in dorsal regions of the embryo. We test these competing hypotheses using mutant alleles of *dl* and conclude that Dl/Cact binding in dorsal nuclei prevents DNA binding, suggesting that further imaging of Cact may be needed to fully understand Dl-dependent gene expression. This result reveals a Dl gradient that has greater dynamic range, spatial range, robustness, and precision than previously understood (Al Asafen et al., 2020; Liberman et al., 2009; O'Connell & Reeves, 2015; Reeves et al., 2012; Schloop et al., 2025).

Results

Quantification of Dl Mobility Reveals a Dorsal-to-Ventral (DV) Gradient

To measure the mobility of Dl in the embryo, we performed Raster Image Correlation Spectroscopy (RICS) analysis on embryos carrying a monomeric GFP-tagged Dl (Carrell et al., 2017) and an H2Av-RFP construct in a *dl* heterozygous background (hereafter referred to as Dl-GFP embryos; see Materials and Methods). We performed RICS analysis in different locations along the DV axis (Fig. 1A) of nuclear cycle 12-14 embryos, when the Dl gradient is clearly defined and detectable. Specifically, we rapidly imaged small (pixel size ≤ 0.1 μm, 256×256 pixels; see Methods) regions of the embryo (Fig. 1B, Fig. S1A-D and Movies S1-3) and calculated 2D autocorrelation functions (ACFs; Fig. 1B and Equation 1 in Materials and Methods). The ACFs each have a fast (ξ) and slow (η) direction due to the rapid movement and line retracing of the confocal scan, respectively (Fig. 1C,D). We then fit a one-component, pure diffusion model to these ACFs (Fig. 1C and Equation 2 in Materials and Methods; see also Supplemental Information), which allowed us to estimate apparent diffusivities. We found that the apparent Dl diffusivity varied with the nuclear-to-cytoplasmic ratio (NCR) of Dl-GFP intensity, which we take as a proxy for position along the DV axis of the imaged region because embryos were mounted in random DV orientations (Fig. 1A). In particular, the apparent diffusivity was lower on the ventral side of the embryo than on the dorsal side (Fig. 1E). To test whether this trend is statistically significant, we used linear regression, and found the slope of the apparent diffusivity from ventral-to-dorsal to be statistically different from zero (p-value < 10^{-4}; Fig. 1E).

Considering that, on the ventral side of the embryo, Dl is predominantly located in the nucleus, whereas on the dorsal side, Dl is predominantly cytoplasmic, it is possible that the spatial variation in the diffusivity arises from differences in the behavior of nuclear and cytoplasmic Dl. Therefore, we segmented the nuclei and calculated the ACF for the nuclei and the cytoplasm separately (see Supplemental Information). We found a ventral-to-dorsal trend in the apparent diffusivity of nuclear-localized Dl-GFP, as estimated by fitting to the pure diffusion model (p-value < 10^{-4}, Fig. 1F). However, the apparent cytoplasmic diffusivities showed no statistically significant trend in spatial variation (p-value 0.6; Fig. 1G). These results suggest that the observed gradient in Dl mobility is specific to nuclear-localized Dl.

We reasoned that the gradient in the mobility of nuclear-localized Dl could be dependent on Toll signaling, which not only favors the dissociation of the Dl/Cact complex, but also phosphorylates Dl and increases its affinity for the nucleus (Drier et al., 1999, 2000; Gillespie & Wasserman, 1994; Whalen & Steward, 1993). To this end, we performed RICS analysis on three mutant lines with "ventral-like" ($Toll^{10B}$; Schneider et al., 1991), "lateral-like" ($Toll^{r4}$; Schneider et al., 1991), or "dorsal-like" ($pll^{2/7}$; Anderson and Nüsslein-Volhard, 1984) levels of nuclear Dl-GFP (Fig. S1E-G). If the spatial gradient in Dl movement depends on Toll signaling, then we would expect $Toll^{10B}$ embryos to have the lowest apparent diffusivity, while $Toll^{r4}$ and $pll^{2/7}$ embryos

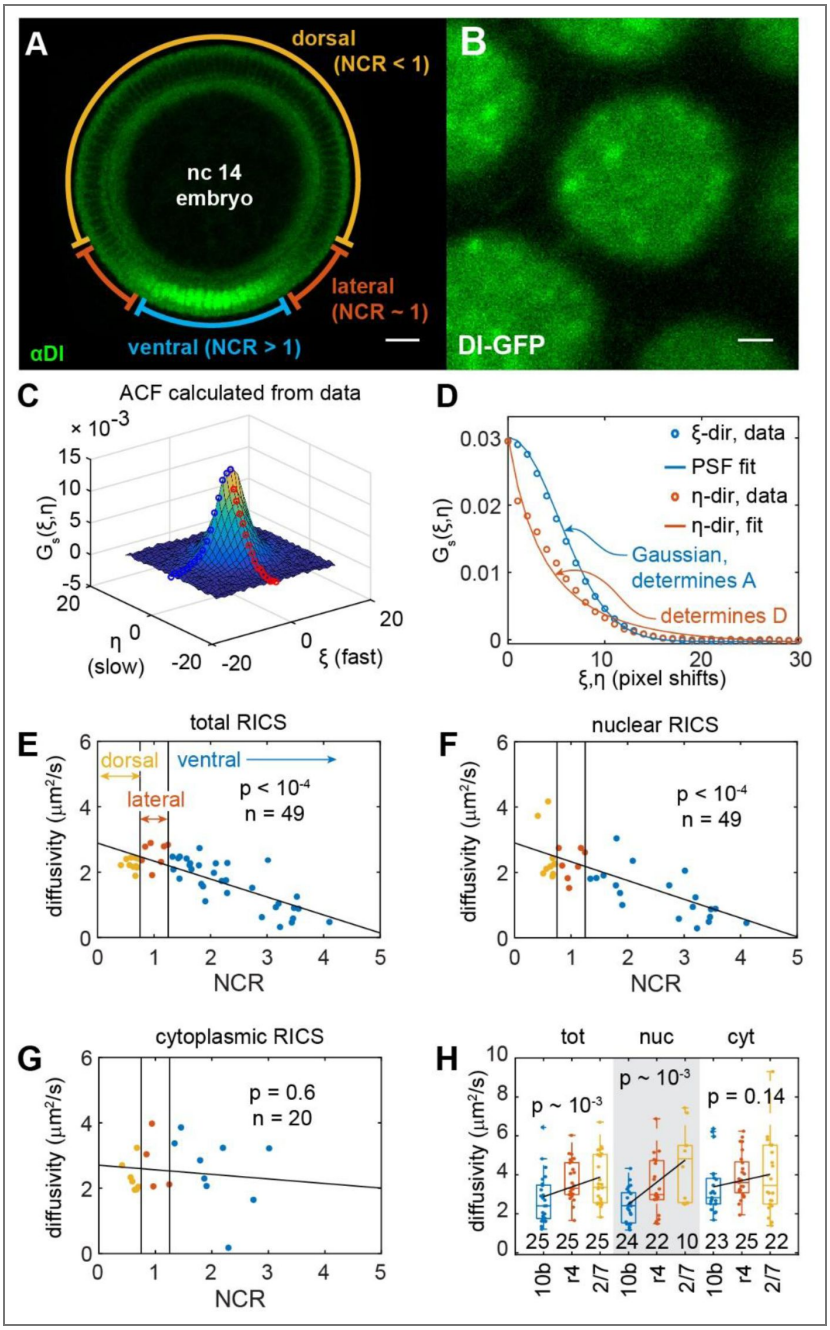

Figure 1. RICS analysis reveals a dorsal-ventral asymmetry in the mobility of Dl.

(A) Representative image of the Dl gradient in an nc 14 embryo. Scale bar = 25 μm. (B) Representative image of Dl-GFP used for RICS analysis. Scale bar = 1 μm. (C,D) Plots of the autocorrelation function (ACF) of the image in A. (C) 3D plot of the ACF. Blue and red open circles represent the slice of the 3D surface for the fast and slow directions, respectively. (D) Plot of the fast and slow slices of the 3D ACF. Blue and red open circles (experimental data) correspond to those found in (C). The experimental data (open circles) are fit using a diffusion model (solid curves). The data and fit are separated into two components, the "fast" (ξ, blue) and "slow" (η, orange) directions. (E-G) Plots of the diffusivity of Dl-GFP vs NCR, measured using RICS on the entire imaging frame (nuclear plus cytoplasmic) (E), nuclear regions only (F), or cytoplasmic regions only (G). (H) Boxplot of the diffusivity of Dl-GFP in mutant embryos measured using RICS on the entire imaging frame (nuclear plus cytoplasmic) ("tot"; left side), nuclear regions only ("nuc"; center, gray), or cytoplasmic regions only ("cyt"; right side). In (E-H), blue represents ventral/"ventral-like", orange represents lateral/"lateral-like", and yellow represents dorsal/"dorsal-like" measurements. Solid dots represent individual measurements. Black lines represent a linear regression fitted to the data. *p*-values for the slope of the trendline being zero are indicated on the graph. Sample sizes indicated on graph.

would have higher apparent diffusivities. Accordingly, we found the apparent diffusivity of total (nuclear + cytoplasmic) Dl-GFP is correlated to the strength of Toll signaling across the mutants (Fig. 1H). Additionally, linear regression revealed a ventral-to-dorsal trend (p-value 10^{-3}; Fig. 1H; left side). Similarly, the apparent diffusivity of nuclear Dl-GFP varies across these Toll signaling mutants with a statistically significant trend (p-value 10^{-3}; Fig. 1H, center). In contrast, we did not see a variation in apparent cytoplasmic Dl-GFP diffusivity in the mutants (p-value 0.14; Fig. 1H, right side). It should be noted that these uniform Toll signaling mutants lack a shuttling mechanism that concentrates Dl on the ventral side of wildtype embryos (Carrell et al., 2017), and as such, the NCR observed in these mutants cannot be used as a direct positional variable for comparing mutants to wild type. For this reason, we presented the mutant results as boxplots to highlight overall trends rather than position-matched values. These results suggest that the variation of mobility along the DV axis is downstream of Toll signaling.

The Gradient of Apparent Diffusivity is Due to Immobilized Dl in the Nucleus

Given that Dl is a transcription factor, it is likely that there are at least two pools of Dl: a freely diffusing pool, and a DNA-bound (immobile) pool. As such, it is possible that the diffusivity is constant, and the observed trend in apparent diffusivity, as inferred by the pure diffusion model, would in fact be a trend in the immobile fraction of Dl. For example, if a significant pool of immobile Dl exists, it would lower the apparent diffusivity, as estimated by a pure diffusion model.

To investigate this possibility, we fit a two-component diffusion model (Equation 3 in Materials and Methods) to the ACFs described above. In the two-component model, Dl could be in two states: freely diffusible and immobilized (Fig. 2A; see Supplemental Information for more details). Thus, an additional adjustable parameter is required: the fraction of immobilized Dl, Φ. To avoid over-fitting, when using the two-component model, we fixed the diffusivity to be 3 $\mu m^2/s$, consistent with the cytoplasmic diffusivity measured above (Fig. 1F, left side). In general, we found the two-component model fit the ACFs better than the one-component model (Fig. 2B). Furthermore, we found that Φ_{nuc}, the fraction of immobilized Dl in the nuclei, varies along the DV axis, with a statistically significant linear trend in NCR (p-value < 10^{-4}; Fig. 2C). In contrast, in the cytoplasm, roughly 10-20% of Dl was immobilized (Φ_{cyt}) in wildtype embryos, and the variation in this fraction along the DV axis lacked a statistically significant trend (p-value 0.08; Fig. 2D).

In the previously described Toll signaling mutants, the immobile fraction of nuclear Dl-GFP was statistically highly correlated with Toll signaling strength (p-value < $10^{-4;}$ Fig. 2E, left side). The immobile fraction in the cytoplasm in the Toll signaling mutants did not rise to a statistically significant trend (p-value 0.06; Fig. 2E, left side).

Taken together, our RICS data from both wildtype and mutant embryos are indicative of a two-component system where a pool of Dl is immobilized, and that the immobile pool, specifically in the nuclei, is highly correlated to Toll signaling. If the immobile pool represents Dl/DNA binding, then the expectation for a transcription factor interacting with DNA is that the concentration of immobile Dl should be a saturating, increasing function of total nuclear Dl concentration. In contrast, in such a saturating system, the *fraction* of immobile Dl, Φ, is expected to decrease (or, at best, remain constant) with increasing nuclear total Dl concentration. However, we are observing the opposite trend (Φ being positively correlated with nuclear Dl), suggesting that the variation in the immobile Dl pool along the DV axis is dictated by more than simply the nuclear Dl concentration.

Dorsal/DNA binding exhibits a spatial gradient

Our RICS results suggest that the spatial variation in nuclear Dl movement is due to a population of immobilized Dl-GFP on the ventral side of the embryo. To test whether the immobilized Dl in the nuclei is due to DNA binding, and whether there is a spatial gradient in DNA binding, we used cross-correlation RICS (ccRICS; Digman et al., 2009) to measure the extent to which Dl (Dl-GFP)

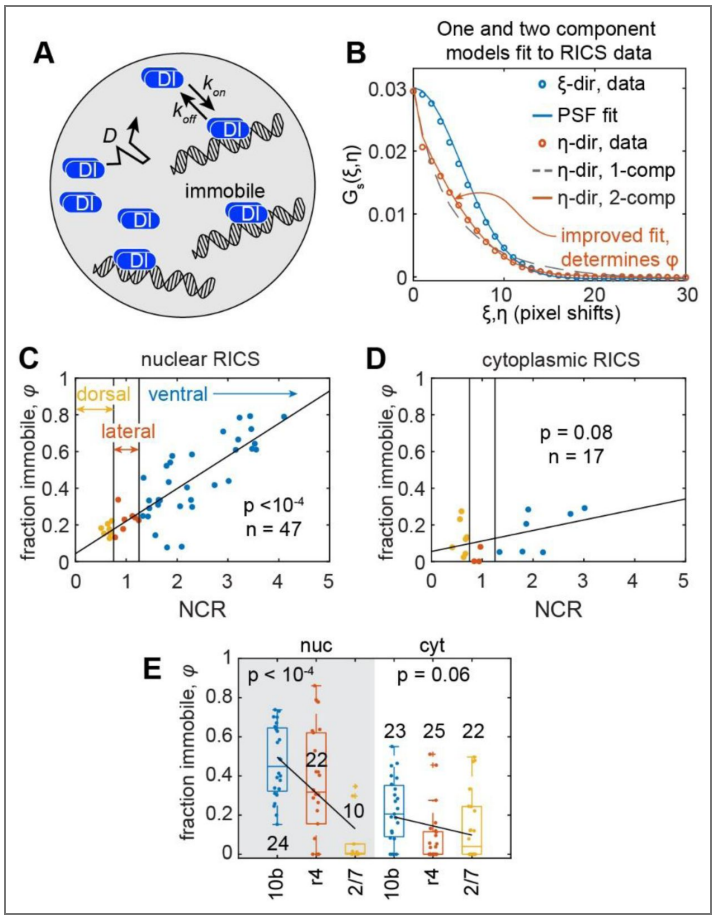

Figure 2. One- and two-component diffusion models quantify the relationship between DNA binding and mobility of Dl.

(A) Illustration of the two-component model. Dl can diffuse and reversibly bind DNA. Dl bound to DNA is immobile. In contrast to the one-component diffusion model, in which Dl is freely diffusible and does not bind to DNA. (B) Comparison of one-component (dashed gray curve) and two-component (solid orange curve) diffusion models fit to the slow direction of the experimental RICS data (orange open circles). (C,D) Plots of the fraction of immobilized Dl (φ) vs. NCR measured using RICS on nuclear regions only (C) or cytoplasmic regions only (D). (E) Boxplot of φ in mutant embryos measured using RICS on nuclear regions only ("nuc"; left side, gray) or cytoplasmic regions only ("cyt"; right side). In (C-E), blue represents ventral/"ventral-like", orange represents lateral/"lateral-like", and yellow represents dorsal/"dorsal-like" measurements. Solid dots represent individual measurements. Black lines represent a linear regression fitted to the data. *p*-values for the slope of the trendline being zero are indicated on the graph. Sample sizes indicated on graph.

and Histone (H2Av-RFP) may be bound to the same physical structure (in this case, DNA). The ratio of the cross-correlation function (CCF) amplitude (Fig. 3A,B) to the ACF amplitude in the red channel (H2Av-RFP channel; Fig. 3C) is proportional to the fraction of Dl bound to DNA, ψ (see Supplemental Information)(Rippe, 2000; Weidemann et al., 2002). Note that it is possible for the CCF amplitude to be negative (Dl-GFP avoidance of H2Av-RFP), in which case, the fraction ψ could be viewed as zero. We found ψ has a statistically significant linear trend with NCR (p-value < 10^{-4}; Fig. 3D). In some cases with high ψ, the overlap between Dl-GFP and H2Av-RFP can be seen visually (Fig. S2A and Movie S4). Furthermore, in dorsal regions, the correlation between histone and Dl is indistinguishable from zero. In these cases, the low correlation can be seen as the lack of peak in the CCF (Figs. 3B, S3B,C).

In the Toll signaling mutant embryos, ψ is also correlated with the levels of Toll signaling with a statistically significant trend (p-value < 10^{-4}; Fig. 3E). Furthermore, ψ is indistinguishable from zero in $pll^{2/7}$ mutants. Note that, as with the Dl diffusivity, there may not be a direct comparison between ψ in the uniform Toll signaling mutants and the corresponding locations in wildtype embryos.

To test whether ccRICS is an appropriate assay to detect Dl/DNA binding, we made a GFP-fused allele of *dl* in which arginine 63 has been replaced by a cysteine (dl^{R063C}-*gfp*), which is in the highly conserved DNA binding portion of the Rel homology domain and has been shown to severely reduce Dl-mediated gene expression (Govind et al., 1996; Isoda et al., 1992). As this allele is antimorphic (Isoda et al., 1992), we used a *nos*-Gal4 line to drive the expression of UAS-dl^{R063C}-*gfp* (Brand & Perrimon, 1993) and overexpressed it in a maternal background of one copy of transgenic *dl-mGFP* and zero copies of endogenous *dl* (see Materials and Methods). To directly compare to a wildtype control, we also created a Gal4/UAS-driven wildtype allele of *dl* fused to *gfp* (UAS-dl^{wt}-*gfp*). As predicted, the UAS-dl^{R063C}-*gfp* allele had a statistically lower value of ψ on the ventral side than the wildtype control (p-value 10^{-3}; Fig. 3F, left side). In contrast, both alleles had a low value of ψ on the dorsal side (p-value 0.3; Fig. 3F, right side). These results are consistent with ψ being a measure of Dl/DNA binding.

Overall, the findings that both the DNA-bound pool and the immobilized pool of nuclear Dl-GFP are correlated to both Toll signaling and the NCR suggest that DNA binding of Dl may be responsible for its overall lowered mobility on the ventral side of the embryo. Furthermore, as mentioned in the previous section, the trends of immobile fraction, Φ, and fraction of Dl/DNA interactions, ψ, both being positively correlated with nuclear Dl concentration is the opposite of what would be expected for a saturating system consisting only of transcription factor/DNA interactions.

Dl Exhibits DV Variation in Nuclear Export Propensity

Our RICS analysis revealed that Dl movement is lowest on the ventral side, where it is primarily nuclear localized and a significant fraction is immobile, and highest on the dorsal side, where it is primarily cytoplasmic. Thus, we reasoned that the ability of Dl to exit the nucleus could also vary spatially. To determine whether there is spatial variation in Dl movement into or out of the nucleus, we used Pair Correlation Function (pCF) analysis to measure any restriction of movement of Dl-GFP across the nuclear envelope (Digman & Gratton, 2009, 2011; Hinde et al., 2010). Here it is important to state the term "movement" can be ambiguous, and in other sections, movement refers to apparent diffusion, which is random, passive motion inside the nucleus or cytoplasm In this section, movement refers to the propensity of Dl to exit the nucleus.

In contrast to RICS, which uses 2D raster scans of the embryo, pCF requires line scans. For our purposes, these line scans cross one or more nuclei (white arrows in Fig. 4A, top row). Pairs of pixels, Δx = 6 pixels apart, are then correlated over time to calculate the pCF carpet (Fig. 4A, bottom panels). A positive correlation occurs only when a Dl-GFP molecule that is detected in a pixel at position $x = x_1$ and time point t_1 is detected again Δx = 6 pixels to the right at time point t_2. Statistically, all occurrences of positive correlations starting at $x_1$and having a time difference of Δt

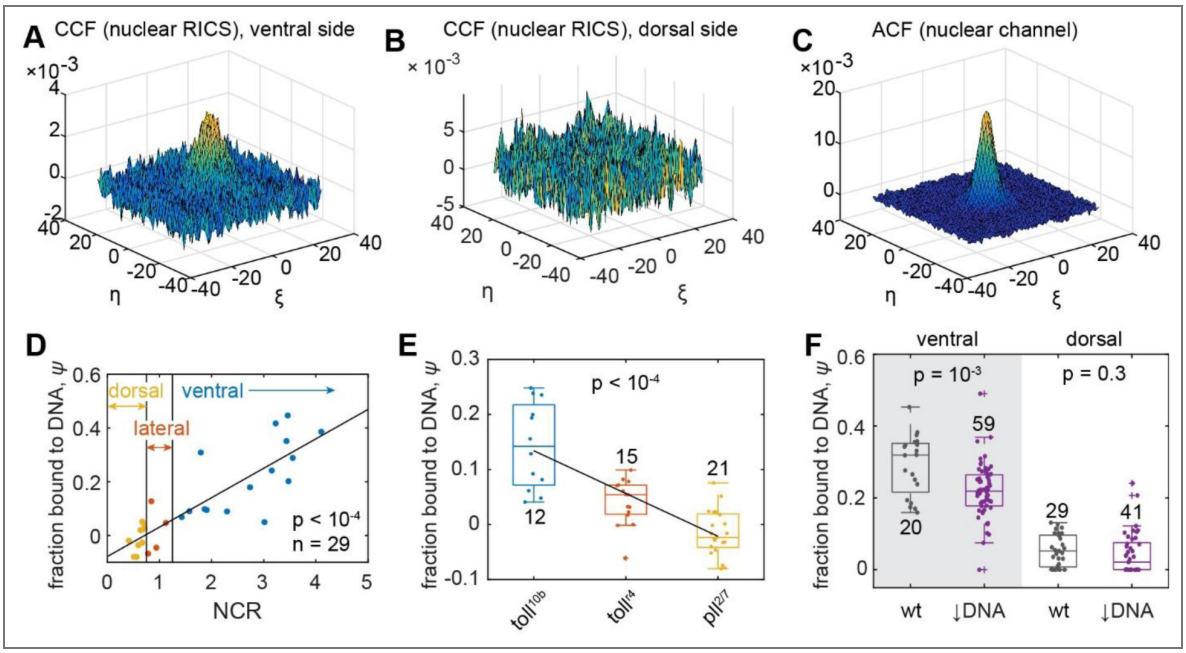

Figure 3. **Cross-correlation RICS analysis of DNA-bound Dl.**

(A,B) Cross-correlation between Dl-GFP and H2Av-RFP, with nuclear mask, on the ventral side (A) or the dorsal side (B). (C) Example of autocorrelation function of H2Av-RFP, with nuclear mask. (D) Plot of ψ, the fraction of Dl bound to DNA, in wildtype embryos vs. NCR. (E) Boxplot of ψ in Toll signaling mutant embryos. In (D,E), blue represents ventral/"ventral-like", orange represents lateral/"lateral-like", and yellow represents dorsal/"dorsal-like" measurements. Solid dots represent individual measurements. Black lines represent a linear regression fitted to the data. *p*-values for the slope of the trendline being zero are indicated on the graph. (F) Boxplot of ψ, the fraction of Dl bound to DNA, in either wildtype (wt) embryos or embryos overexpressing a mutated form of Dl (R063C) with reduced DNA binding (↓DNA). Left side of plot (gray): ventral side; right side of plot (white): dorsal side. *p*-values for differences in means of the distributions are indicated on the graph. In (D-F): Sample sizes indicated on graph.

= $t_2 - t_1$ are averaged over 200,000 scans of the line across the nuclei, resulting in a value on the pCF carpet at coordinate (x_1, Δt). To ensure robustness of the data, pCF carpets were also calculated for Δx = 7 or 8 pixels, as well as for pairs of pixels in the right-to-left direction.

After visual inspection of the pCF carpets, we noticed that pixel locations just to the left of the nuclear membrane aligned with either zero correlation (green bars, Fig. 4A), in which no positive correlation is detected over the time course of the experiment, or delayed correlation (orange arches, Fig. 4A), in which the earliest positive correlations are detected much later compared to other pixel locations. These visual inspections suggested that Dl-GFP molecules in the nucleus either failed to cross the nuclear membrane or could not do so immediately. To quantify this, we calculated the Movement Index (MI) for each embryo, which represents the degree of Dl-GFP movement across the nuclear envelope (see Materials and Methods). A high movement index suggests that Dl-GFP can cross the nuclear envelope, which is represented by an arch in the pCF carpet (demarcated by orange, dashed lines in Fig. 4A). In contrast, a low movement index suggests that Dl-GFP movement into or out of the nucleus is blocked, which is represented by a fully black column in the pCF carpet (demarcated by green, solid lines in Fig. 4A). Note that, as pCF tracks the same molecule twice (Digman & Gratton, 2009; Hinde et al., 2010), the MI correlates with the time scale over which an individual Dl-GFP molecule can exit the nucleus, and is not equivalent to a nuclear export rate constant, which is a measure of average nuclear export.

We separated our images into two groups, those with high movement (MI > 0.5) and those with low movement (MI ≤ 0.5). We found that Dl-GFP can move into the nucleus across the spatial regions of the embryo, as the ventral, lateral, and dorsal regions all have a majority of images with high MI values (ventral: 92.86%; lateral: 94.44%; dorsal: 100.00%) (Fig. 4B). However, the ventral and lateral regions have significantly fewer images with high MI values when Dl-GFP is measured leaving the nucleus (ventral: 64.29%; lateral: 72.22%; p<0.07, Chi-squared test with likelihood ratio), suggesting that Dl-GFP movement out of the nucleus is restricted in the ventral and lateral regions of the embryo (Fig. 4B). In contrast, on the dorsal side of the embryo, almost all the images measuring Dl-GFP movement out of the embryo have high MI values (94.44%). To test whether this restricted movement out of the nucleus may be dependent on Toll signaling, we also performed pCF analysis in $Toll^{10B}$, $Toll^{r4}$, and $pll^{2/7}$mutant lines (Fig. S3A), and similarly found that a lower proportion of images in “ventral-like” mutants have high MI values when Dl-GFP movement is measured out of the nucleus ($Toll^{10B}$: 96.15% in versus 72.73% out; p<0.05, Chi-squared test with likelihood ratio) (Fig. 4B). This suggests that the restriction of Dl to exit the nucleus correlates with the spatial gradient in Toll signaling. As Dl/DNA interactions also correlate with Toll signaling, DNA binding may explain our pCF results. For example, it is likely that a Dl-GFP molecule detected by pCF in a ventral nucleus may be bound to DNA initially, implying it will take longer on average to exit the nucleus than a Dl molecule not initially bound to DNA. Therefore, on the ventral side, the time scale on which an individual Dl-GFP molecule exits the nucleus is longer than on the dorsal side (where DNA binding is not happening). This can be true even if the nuclear export rate constants are the same on the ventral side vs the dorsal side. Thus, our pCF results are consistent with a high fraction of immobilized Dl in the nuclei on the ventral side of the embryo.

Analysis of *dl* mutant alleles suggests Cact is present in the nuclei

Our results demonstrate that, on the ventral side, a significant fraction of Dl is bound to DNA, while on the dorsal side, that fraction is statistically indistinguishable from zero. This phenomenon raises the question of how Dl, as a transcription factor, would be present in the nucleus, but not bind to DNA. More generally, we ask what mechanism may cause the fraction of Dl bound to DNA to positively correlate with nuclear Dl concentration, when a mechanism consisting solely of saturating biochemical binding interactions predicts the opposite. As the gradient in Dl/DNA interactions is dictated by Toll signaling, we reasoned that, on the ventral side, Dl/DNA binding may be enhanced by phosphorylation of Dl by Toll. Toll phosphorylation of Dl is known to enhance the affinity of Dl for the nucleus (Fig. 5A’) (Drier et al., 1999), but its effect on DNA binding is unknown. To test this hypothesis, we made another GFP-fused allele of *dl*, this

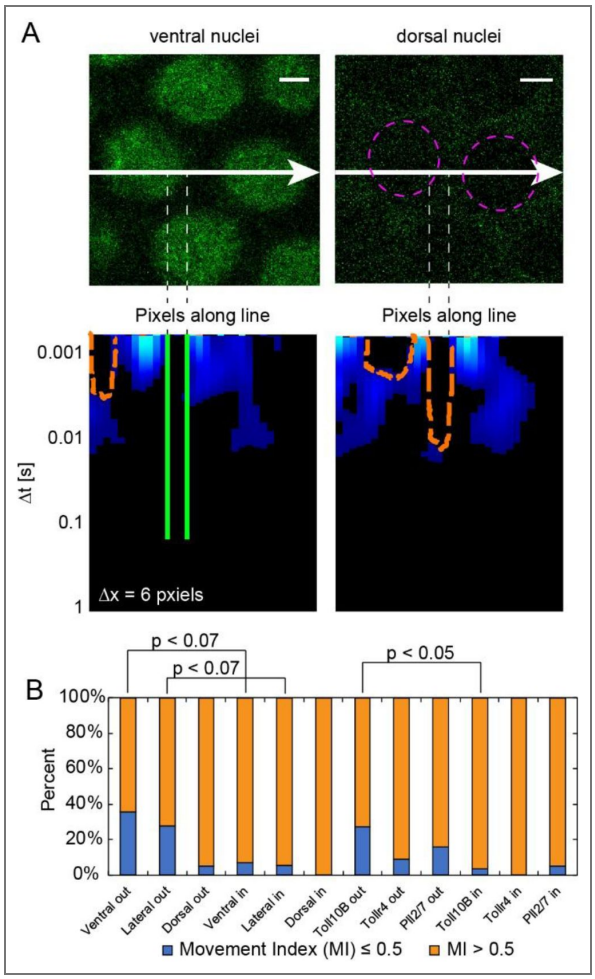

Figure 4. pCF analysis reveals a dorsal-to-ventral asymmetry in nuclear export of Dl.

(A) Representative images of Dl-GFP on th ventral (top left image) and dorsal (top right image) sides of the embryo with their respective pCF carpets (bottom left and bottom right). Scale bar = 2um. White arrows represent the direction and y-coordinate of the pCF line scan. Magenta circles in dorsal side image outline the two nuclei crossed by the line scan. Dashed vertical lines illustrate two cases of locations in the images where a crossing of the nuclear envelope is observed (inside the nucleus to outside). A Dl-GFP molecule observed on the left vertical line (inside the nucleus) may or may not be detected at the location of the right vertical line (outside) at a later time point. Orange, dashed lines in the carpet label arches which indicate delayed Dl-GFP movement, while green, solid lines demarcate black regions of the carpet which indicate no Dl-GFP movement. (B) Percent of embryos that have high (Movement Index (MI) > 0.5, orange) and low (MI ≤ 0.5, blue) Dl-GFP movement either out of (out) or into (in) the nucleus. * denotes p<0.07, ** denotes p<0.05, Chi-squared test with likelihood ratio.

time with an alanine replacing serine at Dl residue 317 (*dl*^{S317A}-*gfp*). This allele has been shown to have reduced Toll-mediated phosphorylation of Dl (Drier et al., 1999). Because Dl acts as a homodimer, and thus, like *dl*^{R063C}-*gfp*, this allele may be antimorphic (Drier et al., 1999), we used the *nos*-Gal4 line to drive the expression of UAS-*dl*^{S317A}-*gfp* (Brand & Perrimon, 1993). As this allele has been shown to drastically reduce the nuclear localization of Dl (Drier et al., 1999), we imaged embryos carrying one copy of this UAS-driven allele and zero copies of wildtype Dl and found that these embryos had no discernible Dl gradient (Fig. S4A). Therefore, to maintain DV polarity so that the ventral and dorsal sides of the embryo could be distinguished, we overexpressed this allele in the background of the BAC recombineered Dl-mGFP construct. We again used the UAS-*dl*^{wt}-*gfp* as a direct wildtype control. As such, if Toll phosphorylation of Dl is responsible for allowing Dl/DNA interactions, then this allele should have reduced DNA binding on the ventral side compared to the wildtype control. However, upon performing ccRICS analysis, we found that the DNA binding of this allele was not statistically distinguishable from the control on the ventral side (Fig. 5B). We note that we cannot completely rule out the hypothesis that Toll signaling has a small effect on Dl/DNA binding, given these embryos expressed the *dl*^{S317A}-*gfp* allele in the background of the BAC recombineered construct.

Alternatively, we reasoned that, on the dorsal side, Dl in the nuclei may be in complex with Cact, preventing it from binding to DNA (Fig. 5A'''), as suggested by our experimental and modeling work (Al Asafen et al., 2020; O'Connell & Reeves, 2015; Schloop et al., 2025). As Dl/Cact interactions are downstream of Toll signaling, this hypothesis would be consistent with the gradient in Dl/DNA interactions being dictated by Toll signaling. Therefore, we made a GFP-fused *dl* allele that has reduced Cact binding by mutating serine 234 to a proline (*dl*^{S234P}-*gfp*)(Drier et al., 2000) and as above, to avoid potential antimorphic effects, we used *nos-Gal4* to overexpress the allele. It has been reported that eliminating the Dl/Cact binding results in a weak gradient of Dl, with Dl significantly entering the nuclei on the Dl side of the embryo (Drier et al., 2000). As such, we imaged embryos carrying one copy of UAS-*dl*^{S234P}-*gfp* without the benefit of the background of the BAC recombineered construct, and found no discernible Dl gradient, similar to the Toll phosphorylation mutant (Fig. S4B). Therefore, to ensure DV polarity of the Dl gradient is maintained, we performed ccRICS on embryos overexpressing this allele in the background of the BAC recombineered Dl-mGFP construct. If the presence of Cact in the dorsal nuclei is responsible for preventing Dl/DNA interactions, then this allele should have increased DNA binding on the dorsal side compared to the wildtype control. Indeed, our ccRICS analysis found that the DNA binding of this allele was greater than the control on the dorsal side (Fig. 5C). The small effect size was likely due to the presence of a wildtype Dl protein in the form of the BAC recombineered Dl-mGFP construct. Indeed, the small effect size may have prevented us from discerning a statistically significant effect of this allele to increase Dl binding on the ventral side (Fig. 5B). Nevertheless, the effect on the dorsal side (Fig. 5C) was statistically significant (p-value $\sim 10^{-3}$). We conclude that the gradient in nuclear Dl mobility is due to Dl/Cact complex in the nucleus; however, we cannot rule out an additional, albeit small, role that Toll phosphorylation may also play. Our previous modeling work has predicted that the presence of Cact in the nucleus affects the spatial range of the Dl gradient and the robustness of gene expression (Al Asafen et al., 2020; O'Connell & Reeves, 2015). Thus, our findings affect the foundation of our understanding of Dl-dependent patterning of the DV axis.

Discussion

In this study, we used fluorescence fluctuation spectroscopy methods to quantify the movement of a BAC-recombineered, GFP-tagged Dl protein in the 1-3 hr old *Drosophila* embryo (Fig. 5A). Our investigations ultimately unveiled a DV asymmetry in the mobility of Dl, which was correlated to a similar DV asymmetry in the ability of Dl to bind to DNA. First, through RICS analysis, we identified variations in Dl's apparent diffusivity along the DV axis within the nucleus. Given the possibility that at least two pools of Dl exist in the nucleus (free vs immobilized), we built a two-component model that accounts for both pools of Dl and found that the DV asymmetry in the fraction of immobilized Dl explained the DV asymmetry in apparent diffusivity. Therefore, to test

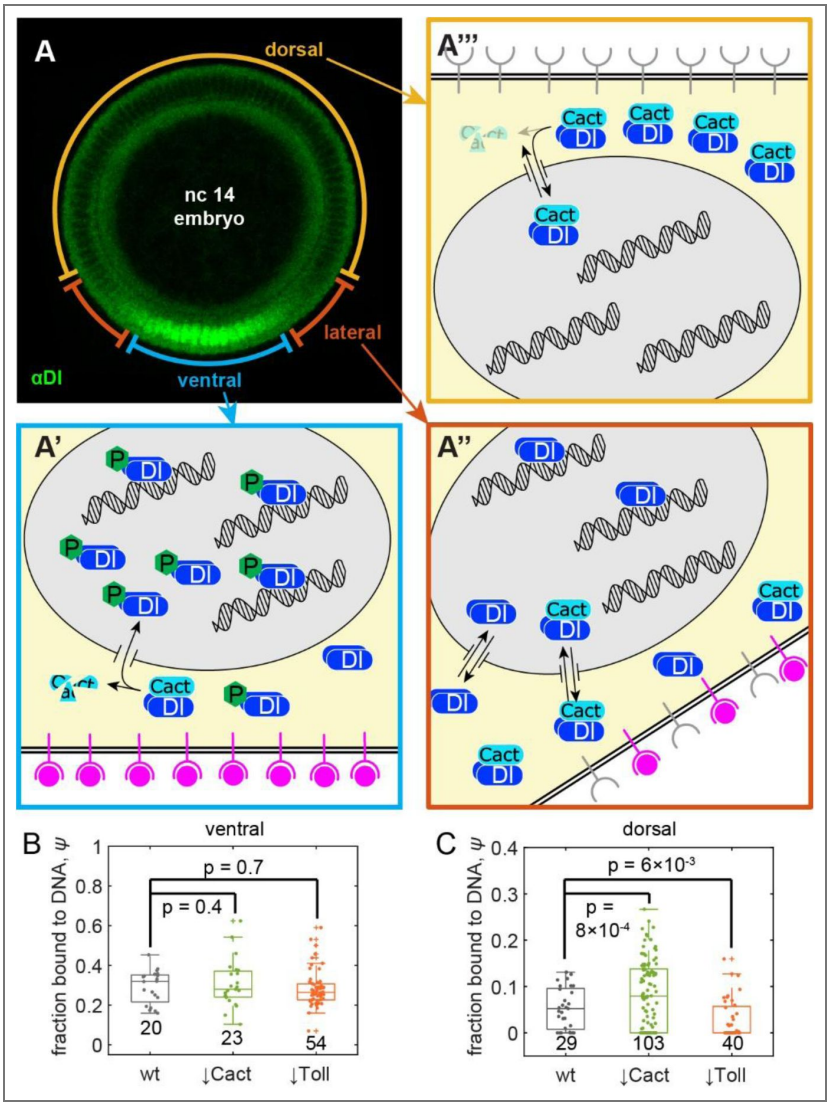

Figure 5. Variation of Dl mobility along the DV axis is due to presence of Cact in the nuclei.

(A) (top left) Depiction of the different embryo domains, ventral (blue region), lateral (orange region), and dorsal (yellow region). Same embryo as in Fig. 1A. (A') Schematic of ventral side of embryo. High levels of activated Toll (magenta receptors) result in the destruction of Cact and phosphorylation of Dl. Free Dl enters the nucleus, so GFP fluorescence is mostly nuclear. Free Dl in the nucleus binds to DNA, which lowers the overall mobility of Dl species, and exits the nucleus at a slow rate. (A'') Schematic of lateral domain of embryo. Lower levels of Toll activation lead to a mixture of free and Cact-bound Dl. Nuclear and cytoplasmic levels of GFP fluorescence are roughly equal. Dl has a higher mobility due to lower fraction of Dl bound to the DNA. Dl exits the nucleus faster than on the ventral side. (A''') Schematic of the dorsal domain of the embryo. Little-to-no free Dl is present, so Dl-GFP fluorescence is mostly cytoplasmic. High mobilities stem from no DNA binding. (B,C) Boxplots of ψ, the fraction of Dl bound to DNA for the UAS-dl^{wt}-*gfp* (control), UAS-dl^{S234P}-*gfp* (reduced Cact binding: ↓Cact), and UAS-dl^{S317A}-*gfp* (reduced Toll phosphorylation: ↓Toll) alleles on the ventral (B) or dorsal (C) sides. The median line for S317A in (C) is located at ψ = 0. Solid dots represent individual measurements. *p*-values for pairwise comparisons to the control are indicated on the graph. Sample sizes indicated on graph.

whether the observed immobilized Dl could be explained by Dl/DNA binding, we used ccRICS to cross-correlate Dl-GFP with Histone-RFP. We indeed found the DV variations in the fraction of immobilized Dl correlated with Dl/DNA binding, with the highest DNA binding on the ventral side. Moreover, the results obtained from pCF showed that there is also variation in the movement of Dl out of the nuclei: on the ventral side, the propensity of Dl to exit the nucleus is not as rapid as it is on the dorsal side. Taken together, our results suggest that there is a DV asymmetry in the efficiency with which Dl can bind to the DNA, and that the restricted nuclear Dl movement on the ventral side of the embryo is explained by a high proportion of DNA-bound Dl.

We identified two plausible explanations that could be causing the DV variation in Dl/DNA interactions. First, Toll-mediated phosphorylation of Dl on the ventral side of the embryo might increase its DNA-binding affinity. Indeed, phosphorylated Dl has increased ability to enter the nucleus (Drier et al., 1999, 2000; Gillespie & Wasserman, 1994; Whalen & Steward, 1993). However, no previous evidence has been shown supporting phosphorylated Dl having an increased affinity for DNA. Second, it is possible that nuclear Dl on the dorsal side is predominantly in complex with Cact, which would result in high average mobility, owing to the fact that it cannot bind DNA (Geisler et al., 1992; Kidd, 1992). In support of this explanation, our recent live imaging of an endogenously-tagged Cact showed that, in *Drosophila* embryos, Cact is present in the nucleus (Schloop et al., 2025). In comparison, mammalian IκB, the homolog of Cact, enters the nucleus to regulate NF-κB dimers, which are then rapidly exported from the nuclei (Arenzana-Seisdedos et al., 1995, 1997; Banerjee & Sen, 2006; Carlotti et al., 2000; Hall et al., 2006; Lisiero et al., 2020; Turpin et al., 1999).

To test these competing hypotheses, we generated two mutant alleles of *dl*, one of which reduced phosphorylation of Dl by Toll (Drier et al., 1999), and the other reduced Dl/Cact interactions (Drier et al., 2000). Using ccRICS, we found that, while the reduced Toll allele exhibited little-to-no change in DNA affinity on the ventral side, the reduced Cact allele did indeed have increased DNA affinity on the dorsal side, consistent with the prediction of the second hypothesis. However, to maintain the DV polarity of the embryo, we expressed these mutant alleles in the background of the BAC recombineered Dl-mGFP construct, such that the effects of these alleles were diluted by the presence of a GFP-tagged wildtype Dl protein. Therefore, while can safely reject the null hypothesis that Cact has no effect on DNA binding, it is possible that our failure to reject the null hypothesis that Toll phosphorylation has no effect on the DNA binding of Dl on the ventral side may be due to this dilution effect.

Genetically, the bulk of the embryos in this study maternally expressed one copy of endogenous Dl and one copy of the BAC-recombineered construct, which presents two caveats. First, it is known that tagging Dl with a fluorescent protein alters its gradient (Reeves et al., 2012), which may in part be due to a lowered diffusivity (Carrell et al., 2017). As such, any raw diffusivity reported here may measure as slightly lower than that of untagged Dl. We do not expect the fraction immobile or the fraction bound to DNA to be affected. A second caveat is that the presence of endogenous Dl may increase the variance of our data. As Dl exists as a dimer (Govind et al., 1992; Isoda & Nüsslein-Volhard, 1994), our measurements are likely to reflect an ensemble average of a tagged/untagged heterodimer mixed with a tagged homodimer at a 2:1 ratio. We do not expect the existence of a mixed population of Dl dimers to alter our main conclusions.

It is thought that the primary role for Cact is to tether Dl to the cytoplasm and prevent nuclear translocation. Indeed, loss of Cact function permits intermediate levels of Dl to enter the nuclei, even on the dorsal side of the embryo (Bergmann et al., 1996; Cardoso et al., 2017; Roth et al., 1991). However, recent studies have discovered multiple functions for Cact, including positive roles in the formation of the Dl gradient. For example, Cact degradation on the ventral side of the embryo creates a driving force for a ventrally-directed net flux of Dl/Cact complex, which has the overall effect of shuttling Dl to the ventral side (Carrell et al., 2017). Furthermore, recent experimental and modeling work has suggested that Cact potentiates nuclear translocation on the ventral side of the embryo (Barros et al., 2021; Cardoso et al., 2017).

In addition to these roles for Cact in establishing the Dl gradient, our experimental results in this study suggest that, on the dorsal side of the embryo, Cact is present inside the nuclei and plays a role in preventing Dl from binding DNA. While this specific finding relates to the dorsal half of the embryo, where Dl levels are low and are expected to have minimal activity in regulating gene expression, knowing whether Dl is in complex with Cact in the dorsal-most nuclei is crucial to our understanding of the Dl gradient. Indeed, our previous fluorescence measurements have revealed a gradient that decays to non-zero basal levels on the dorsal half of the embryo (Liberman et al., 2009; Reeves et al., 2012); such a gradient would have a very limited dynamic range, varying by less than one order of magnitude (O'Connell & Reeves, 2015). In light of our results in this paper, one solution to this problem is to assume all of the Dl on the dorsal side of the embryo is Dl/Cact complex, meaning that the gradient of free Dl would have an unknown overall shape, but would decay to near-zero levels. We have shown that such a free Dl gradient would not only have extended spatial and dynamic ranges, but also superior precision and robustness of gene expression compared to the gradient measured by fluorescence (Al Asafen et al., 2020; Liberman et al., 2009; O'Connell & Reeves, 2015; Reeves et al., 2012). In support of the assumption that all Dl is bound to Cact on the dorsal side, we have recently shown that Cact exhibits dynamics similar to Dl on the dorsal side of the embryo, suggesting that, in both cases, it is predominantly Dl/Cact complex that is being measured (Hiremath et al., 2024; Reeves et al., 2012; Schloop et al., 2025).

Furthermore, our recent experimental work showed that Cact is present in all nuclei and is spatially uniform along the DV axis of the embryo (Schloop et al., 2025). As such, our results in this paper can likely be extended to Dl/Cact interactions in all nuclei, implying that measurements of the Dl gradient based solely on nuclear fluorescence levels are in fact a combination of a spatially graded pool of free (active) Dl and a spatially uniform level of Dl/Cact complex along the entire DV axis. Thus, the "true" Dl activity gradient remains unquantified, and must be determined by deconvolving Dl/Cact complex from free Dl (O'Connell & Reeves, 2015). If all (or nearly all) of the Dl in the dorsal-most nuclei is indeed bound by Cact, the gradient of free Dl, along the entire DV axis, could be recovered by simply subtracting off the basal levels. However, it is likely that some fraction of Dl in the dorsal-most nuclei is free. Thus, to fully understand the positional information carried by the Dl gradient, direct quantification of Dl/Cact complex, perhaps through ccRICS measurements on embryos in which both Dl and Cact are labeled, should be the next step towards gaining future insights into the operation of the highly conserved NF-κB/Dl module. Ultimately, our work highlights the need for quantitative measurements of biophysical parameters to further our understanding of signaling and gene expression, and calls for similar studies in other signaling pathways in embryonic patterning.

Materials and Methods

Fly Stocks and Preparation

Drosophila melanogaster stocks were kept on corn meal molasses food in vials or bottles at 25°C and all crosses were performed at 25°C. *Drosophila* embryos, that were about 1-2 hrs old, were collected and mounted on slides for imaging. Briefly, flies were left to deposit eggs on fresh grape juice agar plates with yeast paste for 30-60 min. Those embryos were then aged further for 30 min at 25°C to reach the desired developmental stage. Those embryos are then brushed from the grape juice agar plates into a mesh basket using a paintbrush and DI water. The embryos were dechorionated using bleach and then washed with DI water (Carrell & Reeves 2009).

dl-mGFP (Dl-GFP) was created by BAC recombineering and $dl^{1.2.5}$ flies were generated by cleaning up dl^{1} via two homologous recombinations with wildtype flies (Carrell et al. 2017). Flies carrying $dl^{1.2.5}$ were crossed to flies carrying H2Av-RFP on the second chromosome (w[*]; P{w[+mC]=His2Av-mRFP1}II.2; BS# 23651) to generate flies that have $dl^{1.2.5}$,H2Av-RFP transgene on the second chromosome. H2Av-RFP,$dl^{1.2.5}$,*dl-mGFP* flies were created by homologous recombination (Carrell et al. 2017). Thus, the "Dl-GFP embryos" analyzed in this study had a maternal genotype of H2Av-RFP,$dl^{1.2.5}$,*dl-mGFP*/*CyO*: one copy of endogenous *dl* and one copy of *dl-*

mGFP. The generation of *Toll*^{r4} and *Toll*^{10B} mutant embryos has been previously described (Stathopoulos et al. 2002). Other *Drosophila* strains were obtained from the Bloomington (BL) stock center, namely *pll*^{2} (e[1] pll[2] ca[1]/TM3, Sb[1] BS# 3111) and *pll*^{7} (e[1] pll[7] ca[1]/TM3, Sb[1]; BS# 3112), and nos-Gal4 (w[1118]; P{w[+mC]=GAL4::VP16-nanos.UTR}CG6325[MVD1]; BS# 4937).

The pUAST plasmids containing *dl* alleles (*dl*^{wt}-*mgfp*, *dl*^{R063C}-*mgfp*, *dl*^{S317A}-*mgfp*, and *dl*^{S234P}-*mgfp*) were prepared by site-directed mutagenesis using appropriate primers with the Q5® Site-Directed Mutagenesis Kit (New England Biolabs Inc., Frankfurt, Germany). All resulting plasmids were confirmed by direct sequencing. The Gal4/UAS overexpression embryos were maternally H2Av-RFP,*dl*$^{1.2.5}$,*dl-mGFP*/*dl*^{4}; *nos*-Gal4/UAS-*dl*^{x}-*mGFP*, where *x* is either the R063C, S317A, or S234P mutation, or wildtype. Thus, these embryos maternally carried zero endogenous copies of *dl*, one BAC-recombineered *dl-mGFP* construct, and one UAS-*dl*^{x}-*mGFP* construct.

Fly Transformation

Drosophila embryos were injected with 0.5 ng/µl of each pUAST construct using the PhiC31 method by GenetiVision (Texas, USA). Transformed flies include insertion on chromosome III. Stocks were established for each of these flies. The flies were then crossed into a dl^{4} heterozygous background (dl[4] pr[1] cn[1] wx[wxt] bw[1]/CyO BS# 7096) and finally crossed with dl1.2.5 flies (Carrell et al., 2017) driven by nos-gal4 (BS# 4937, see above). The females from this cross were kept in a cage and the resulting embryos were used for live imaging.

Mounting and Imaging of *Drosophila* Embryos

Drosophila embryos that were 1-2 hrs old were mounted laterally on a microscope slide using a mixture of heptane glue (Supatto et al. 2009) and two pieces of double-sided tape to prevent sample movement (Carrell & Reeves 2015). The embryos were mounted in random orientations along the DV axis. The DV position of each imaged region was estimated by measuring the Dl nuclear-to-cytoplasmic ratio (NCR) of intensity, which varies predictably with position along the DV axis. We categorized positions with NCRs > 1.25 as ventral, positions with 0.75 < NCR < 1.25 as lateral, and positions with NCR < 0.75 as dorsal (Fig. 1A). Embryos were imaged on either a Zeiss LSM 710 or LSM 900 confocal microscope using a 40x 1.2NA water objective. Embryos in nuclear cycle 12 to 14 were selected using the H2Av-RFP marker. Embryos undergoing cell division (as visualized by the H2Av-RFP marker) were not used in for analysis as cell division alters the endogenous Dl distribution.

For image acquisition consistent with RICS analysis for the data shown in Figs. 1-3, using a Zeiss LSM 710, a 256 x 256 pixel region of interest of the embryo was selected for measurements (Supplemental Figure 1). The pixel size of the region varied from 40 nm to 100 nm to include different numbers of nuclei. The 25 mW 488 nm laser intensity ranged from 0.5% to 3.0% and the 20 mW 570 nm laser intensity ranged from 0.1% to 0.2%. The region of interest was raster scanned with a pixel dwell time of 6.3 µs for 200 frames (total imaging time of approximately 1.5 minutes). For dl-mutants (data shown in Fig. 5) we used Zeiss LSM 900 with a 1024 x 1024 pixel region of interest, with a pixel size of 30 nm (Supplemental Figure 1), having the laser intensity range same as mentioned above for the 10 mW 488 nm laser and the 10 mW 561 nm laser. The region of interest was raster scanned with a pixel dwell time of 2.1 µs for 100 frames (total imaging time of approximately 9 min). The range of imaging parameters is reported in Table S1.

For image acquisition consistent with pCF analysis, a 32×1 line scan through 2 to 4 nuclei was used as the region of interest (Fig. 4A). The pixel size was not set for each image but, instead, varied between 40-100nm according to the region of interest selected. The laser intensities varied as in the RICS imaging. The line was scanned with a pixel dwell time of 6.30µs for 200,000 to 400,000 time points (total imaging time of approximately 1.5 to 3 minutes). The range of imaging parameters is reported in Table S1.

Raster Image Correlation Spectroscopy (RICS) analysis using MATLAB implementation

RICS analysis of time series images is briefly described here (see Supplemental Information for more details). For each frame *j* (of size 256×256 or 1024×1024 pixels) in the Dl-GFP channel, the scanning ACF, $G_j(\xi, \eta)$, was computed according to the following for all pixel shifts ξ, η:

$$G_j(\xi,\eta) = \frac{\langle I_j(x,y) I_j(x+\xi, y+\eta)\rangle}{\langle I_j(x,y)\rangle^2} - 1, \tag{1}$$

where $I_j(x, y)$ is the intensity of frame *j* at pixel coordinates (x, y) and the angle brackets denote ensemble average in both *x* and *y*. In practice, $G_j(\xi, \eta)$ is evaluated using the fast Fourier transform method (Digman & Gratton, 2011). The final ACF for total RICS, $G_s(\xi, \eta)$, was computed as the average of $G_j(\xi, \eta)$ for all frames *j* in the time series. Cross-correlation functions were computed in a similar way, except $I_j(x + \xi, y + \eta)$ was replaced by the analogous array from the H2Av-RFP channel, and the $\langle I_j(x, y)\rangle^2$in the denominator was replaced by the product of the average intensity in the Dl-GFP channel and the average intensity in the H2Av-RFP channel.

Fitting models to the ACFs

The one component diffusion model for the RICS ACF is (Fig. 1D-F; Digman et al., 2005b):

$$G_s^{1c}(\xi,\eta;A,B,D,w_0) = \frac{(A-B)\exp\left(-\frac{(r/w_0)^2}{1+4D\tau/w_0^2}\right)}{(1+4D\tau/w_0^2)\sqrt{1+4D\tau/w_z^2}} + B, \tag{2}$$

where $r = \Delta r\sqrt{\xi^2+\eta^2}$, $\tau = \tau_p\xi + \tau_\ell\eta$, Δr is the pixel size in microns, τ_p and τ_ℓ are the pixel dwell time and line scan time in seconds, respectively, and $w_0$and $w_z$are the waist sizes of the point spread function in the planar and axial directions, respectively. The two component diffusion/binding model is a linear combination of two instances of Equation (2):

$$\begin{aligned} &G_s^{2c}(\xi,\eta;A,B,\phi,w_0) \\ &= (A-B)\left[\phi G_s^{1c}(\xi,\eta;1,0,0,w_0) + (1-\phi)G_s^{1c}(\xi,\eta;1,0,3,w_0)\right] + B, \end{aligned} \tag{3}$$

where Φ is the fraction of Dl-GFP that is immobilized, in the first term, *D* is held fixed at zero, and in the second term, *D* is held fixed at 3 μm^2/s. Within both terms, G_S^{1c} is normalized such that $A = 1$ and $B = 0$, because the *A* and *B* parameters are otherwise present in Equation (3).

Models of the ACF were fit to the ACFs calculated from the total, nuclear, or cytoplasmic data in two steps. First, the fast direction of the ACF ($\eta = 0$) was used as target to fit $G_S^{1c}(\xi, 0; A, B, 0, w_0)$, that is, Equation (2) with $\eta = 0$ and $D = 0$. The shape of this function is purely Gaussian and approximates the point spread function (PSF). This fit is highly robust, and performing this fit first allows for accurate estimation of the parameter *A*. Two parameters, the PSF waist size, w_0, and the background level, *B*, are theoretically fixed; however, we allowed them to vary slightly from their theoretical values of 0.25 μm and zero, respectively, for robustness of fit.

In the second step, with *A* from the first step fixed, either Equation (2), for the one-component model, or Equation (3), for the two component model, was fit to $G_s(\xi, \eta)$ using least squares and varying *B*, *D*, w_0 or *B*, Φ, w_0, respectively. The parameters Δr, τ_p, τ_ℓ, w_z were microscope parameters and considered fixed. More information can be found in the Supplemental Information.

Pair Correlation Function (pCF) analysis using SimFCS software

Acquisitions were taken of 200,000 scans of a line 32 pixels across (pixel size 0.5 µm), with a pixel dwell time of 6.3 µs and a line time of 0.47 ms, on either the dorsal, lateral, or ventral sides of nc 14 embryos. To ensure minimal movement of nuclei occurred during the line scan aquisition, 512×512 images were taken before and after each acquisition, where the middle y-coordinate of these images corresponded to the location of the line scan (white arrows in Fig. 4A). pCF analysis of the collected line scans was performed using the SimFCS software (Digman et al, 2005; *https://www.lfd.uci.edu/globals/*) as described in Clark and Sozzani, 2017. Three pixel distances of 6, 7, and 8 pixels were used as technical replicates to account for differences in sizes of nuclei. If Dl-GFP showed movement out of/into a majority of nuclei (no black region or black arch in the pCF carpet), that image was assigned a movement index of 1. Otherwise, if the majority of Dl-GFP showed no movement (black vertical region in the pCF carpet), that image was assigned a movement index of 0 (Fig. 4A). The 3 technical replicates were then averaged for each biological replicate. The analysis was repeated for the line scan in the reverse direction, resulting in 6 total technical replicates per image.

Quantification and statistical analysis

Non-linear least squares was used to fit Equation (2) to the RICS ACFs. The fitted diffusivity value is *t*-distributed, and a standard error for the diffusivity (radius of a 68% confidence interval) was calculated. With the exception of five time course image stacks of nuclear RICS either on the dorsal side of wildtype embryos, or in $pll^{2/7}$ embryos (the two cases in which nuclear intensity is very low), for all fitted diffusivities, the standard error was less than 4 $\mu m^2/s$. This was used as a filter for the data; the five time course image stacks in which the standard error was greater than 4 $\mu m^2/s$ were removed from the analysis.

For the diffusivity of Dl calculated by RICS (Fig. 1D-F), the ccRICS data (ratio of amplitudes; Fig. 3C,D), and for the correlation between nuclear diffusivity and ϕ (Fig. 4E), simple linear least squares regression was applied. The slope of the regression trend line is t-distributed with *n*-2 degrees of freedom, where *n* is the number of data points. Reported *p*-values are for *t*-tests with the null hypothesis that the slope is zero.

For the pCF data (Fig. 2), a Chi-squared test with likelihood ratio was used to test if the proportion of Movement Index (MI) values that were less than 0.5 was different for movement measured into the nucleus vs movement measured out of the nucleus. The Chi-squared test was performed using JMP software (*https://www.jmp.com/*).

For all tests, a p-value less than 0.05 was considered significant, and for the Chi-Squared test we also consider the two p-values that were less than 0.07 as significant (Fig. 2). The statistical tests performed on each sample are listed in the Results text as well as the figure legends. Sample sizes are indicated in the figures. Means and standard errors are reported in the Results.

Data availability

Imaging data will be available in the Texas Data Repository. RICS analysis code available on Zenodo at 10.5281/zenodo.15595664.

Acknowledgements

The authors acknowledge the use of the Cellular and Molecular Imaging Facility (CMIF) at North Carolina State University, which is supported by the State of North Carolina and the National Science Foundation.

Additional files

Movie S1.

Movie S2.

Movie S3.

Movie S4.

Supplemental text.

Additional information

Funding

Funder	Grant reference number	Author
National Science Foundation (NSF)	CBET-1254344	Gregory T Reeves Hadel Al Asafen
National Science Foundation (NSF)	DGE-1252376	Natalie M Clark
National Science Foundation (NSF)	MCB-1856654	Etika Goyal Sadia Siddika Dima Gregory T Reeves
National Science Foundation (NSF)	MCB-1413044	Thomas Jacobsen
National Science Foundation (NSF)	CBET-2313692	Hung-Yuan Chen
National Science Foundation (NSF)	MCB- 1453130	Rosangela Sozzani
HHS | National Institutes of Health (NIH)	R21HD092830	Gregory T Reeves
HHS | National Institutes of Health (NIH)	R01GM151409	Gregory T Reeves Sadia Siddika Dima

Author ORCID iDs

Hadel Al Asafen: https://orcid.org/0000-0003-0826-9816
Natalie M Clark: https://orcid.org/0000-0003-0988-321X
Etika Goyal: https://orcid.org/0000-0001-8934-7948
Sadia Siddika Dima: https://orcid.org/0009-0008-3558-9093
Hung-Yuan Chen: https://orcid.org/0009-0006-5827-8197
Rosangela Sozzani: https://orcid.org/0000-0003-3316-2367
Gregory T Reeves: https://orcid.org/0000-0003-0836-7766

References

Al Asafen H., Bandodkar P. U., Carrell-Noel S., Schloop A. E., Friedman J., Reeves G. T. (2020) Robustness of the Dorsal morphogen gradient with respect to morphogen dosage. *PLOS Computational Biology* **16**:e1007750 https://doi.org/10.1371/journal.pcbi.1007750 | PubMed

Anderson K. V, Bokla L., Nüsslein-Volhard C (1985) Establishment of dorsal-ventral polarity in the Drosophila embryo: the induction of polarity by the Toll gene product. *Cell* **42**:791-798 https://doi.org/10.1016/0092-8674(85)90275-2 | PubMed

Anderson K. V, Jürgens G., Nüsslein-Volhard C (1985) Establishment of dorsal-ventral polarity in the Drosophila embryo: Genetic studies on the role of the Toll gene product. *Cell* **42**:779-789 https://doi.org/10.1016/0092-8674(85)90274-0 | PubMed

Anderson K. V, Nüsslein-Volhard C (1984) Information for the dorsal--ventral pattern of the Drosophila embryo is stored as maternal mRNA. *Nature* **311**:223-227 https://doi.org/10.1038/311223a0 | PubMed

Arenzana-Seisdedos F., Thompson J., Rodriguez M. S., Bachelerie F., Thomas D., Hay R. T (1995) Inducible nuclear expression of newly synthesized I kappa B alpha negatively regulates DNA-binding and transcriptional activities of NF-kappa B. *Mol Cell Biol* **15**:2689-2696 https://doi.org/10.1128/mcb.15.5.2689 | PubMed

Arenzana-Seisdedos F., Turpin P., Rodriguez M., Thomas D., Hay R. T., Virelizier J. L., Dargemont C (1997) Nuclear localization of I kappa B alpha promotes active transport of NF-kappa B from the nucleus to the cytoplasm. *J Cell Sci* **110**:369-378 https://doi.org/10.1242/jcs.110.3.369 | PubMed

Banerjee D., Sen R. (2006) Cellular Dynamics of NF-κB Associated Proteins. In: Liou H-C. (Ed). *NF-κB/Rel Transcription Factor Family* Springer US. pp. 41-50 https://doi.org/10.1007/0-387-33573-0_4

Barros C. D. T., Cardoso M. A., Bisch P. M., Araujo H. M., Lopes F. J. P (2021) A reaction-diffusion network model predicts a dual role of Cactus/IκB to regulate Dorsal/NFκB nuclear translocation in Drosophila. *PLOS Computational Biology* **17**:e1009040 https://doi.org/10.1371/journal.pcbi.1009040 | PubMed

Belvin M. P., Anderson K. V (1996) A Conserved Signalig Pathway: The Drosophila Toll-Dorsal Pathway. *Annual Review of Cell and Developmental Biology* **12**:393-416 https://doi.org/10.1146/annurev.cellbio.12.1.393 | PubMed

Belvin M. P., Jin Y., Anderson K. V (1995) Cactus protein degradation mediates Drosophila dorsal-ventral signaling. *Genes Dev* **9**:783-793 https://doi.org/10.1101/gad.9.7.783 | PubMed

Bergmann A., Stein D., Geisler R., Hagenmaier S., Schmid B., Fernandez N., Schnell B., Nüsslein-Volhard C (1996) A gradient of cytoplasmic Cactus degradation establishes the nuclear localization gradient of the dorsal morphogen in Drosophila. *Mechanisms of Development* **60**:109-123 PubMed | https://doi.org/10.1016/s0925-4773(96)00607-7

Brand A. H., Perrimon N (1993) Targeted gene expression as a means of altering cell fates and generating dominant phenotypes. *Development* **118**:401-415 https://doi.org/10.1242/dev.118.2.401 | PubMed

Cardoso M. A., Fontenele M., Lim B., Bisch P. M., Shvartsman S. Y., Araujo H. M (2017) A novel function for the IκB inhibitor Cactus in promoting Dorsal nuclear localization and activity in the Drosophila embryo. *Development* **144**:2907-2913 https://doi.org/10.1242/dev.145557 | PubMed

Carlotti F., Dower S. K., Qwarnstrom E. E (2000) Dynamic Shuttling of Nuclear Factor κB between the Nucleus and Cytoplasm as a Consequence of Inhibitor Dissociation. *Journal of Biological Chemistry* **275**:41028-41034 https://doi.org/10.1074/jbc.M006179200 | PubMed

Carrell S. N., Connell M. D. O., Jacobsen T., Pomeroy A. E., Hayes S. M., Reeves G. T (2017) A facilitated diffusion mechanism establishes the Drosophila Dorsal gradient. *Development* **144**:4450-4461 https://doi.org/10.1242/dev.155549 | PubMed

Chopra V. S., Levine M (2009) Combinatorial patterning mechanisms in the Drosophila embryo. *Briefings in Functional Genomics & Proteomics* **8**:243-249 https://doi.org/10.1093/bfgp/elp026 | PubMed

Daigneault J., Klemetsaune L., Wasserman S. A (2013) The IRAK homolog Pelle is the functional counterpart of IκB kinase in the Drosophila Toll pathway. *PLoS One* **8**:e75150 https://doi.org/10.1371/journal.pone.0075150 | PubMed

Delotto R., Delotto Y., Steward R., Lippincott-schwartz J (2007) Nucleocytoplasmic shuttling mediates the dynamic maintenance of nuclear Dorsal levels during Drosophila embryogenesis. *Development* **4241**:4233-4241 https://doi.org/10.1242/dev.010934 | PubMed

Digman M. A., Brown C. M., Sengupta P., Wiseman P. W., Horwitz A. R., Gratton E (2005) Measuring fast dynamics in solutions and cells with a laser scanning microscope. *Biophys J* **89**:1317-1327 https://doi.org/10.1529/biophysj.105.062836 | PubMed

Digman M. A., Gratton E (2009) Imaging barriers to diffusion by pair correlation functions. *Biophys J* **97**:665-673 https://doi.org/10.1016/j.bpj.2009.04.048 | PubMed

Digman M. A., Gratton E (2011) Lessons in fluctuation correlation spectroscopy. *Annual Review of Physical Chemistry* **62**:645-668 https://doi.org/10.1146/annurev-physchem-032210-103424 | PubMed

Digman M. A., Sengupta P., Wiseman P. W., Brown C. M., Horwitz A. R., Gratton E (2005) Fluctuation correlation spectroscopy with a laser-scanning microscope: exploiting the hidden time structure. *Biophys J* **88**:L33-L36 https://doi.org/10.1529/biophysj.105.061788 | PubMed

Digman M. A., Wiseman P. W., Horwitz A. R., Gratton E (2009) Detecting protein complexes in living cells from laser scanning confocal image sequences by the cross correlation raster image spectroscopy method. *Biophys J* **96**:707-716 https://doi.org/10.1016/j.bpj.2008.09.051 | PubMed

Drier E. A., Govind S., Steward R (2000) Cactus-independent regulation of Dorsal nuclear import by the ventral signal. *Current Biology : CB* **10**:23-26 https://doi.org/10.1016/S0960-9822(99)00267-5 | PubMed

Drier E. A., Huang L. H., Steward R (1999) Nuclear import of the Drosophila Rel protein Dorsal is regulated by phosphorylation. *Genes & Development* **13**:556-568 https://doi.org/10.1101/gad.13.5.556 | PubMed

Entchev E. V, Schwabedissen A., González-Gaitán M. A (2000) Gradient Formation of the TGF-β Homolog Dpp. *Cell* **103**:981-991 https://doi.org/10.1016/S0092-8674(00)00200-2 | PubMed

Geisler R., Bergmann A., Hiromi Y., Nüsslein-Volhard C (1992) cactus, a gene involved in dorsoventral pattern formation of Drosophila, is related to the I kappa B gene family of vertebrates. *Cell* **71**:613-621 https://doi.org/10.1016/0092-8674(92)90595-4 | PubMed

Gillespie S. K., Wasserman S. A (1994) Dorsal, a Drosophila Rel-like protein, is phosphorylated upon activation of the transmembrane protein Toll. *Molecular and Cellular Biology* **14**:3559-3568 https://doi.org/10.1128/MCB.14.6.3559 | PubMed

Govind S., Drier E., Huang L. H., Steward R (1996) Regulated nuclear import of the Drosophila rel protein dorsal: structure-function analysis. *Molecular and Cellular Biology* **16**:1103-1114 https://doi.org/10.1128/mcb.16.3.1103 | PubMed

Govind S., Whalen A. M., Steward R (1992) In vivo self-association of the Drosophila rel-protein dorsal. *Proceedings of the National Academy of Sciences of the United States of America* **89**:7861-7865 https://doi.org/10.1073/pnas.89.17.7861 | PubMed

Gregor T., Wieschaus E. F., McGregor A. P., Bialek W., Tank D. W (2007) Stability and nuclear dynamics of the Bicoid morphogen gradient. *Cell* **130**:141-152 https://doi.org/10.1016/j.cell.2007.05.026 | PubMed

Hall G., Hasday J. D., Rogers T. B (2006) Regulating the regulator: NF-κB signaling in heart. *Journal of Molecular and Cellular Cardiology* **41**:580-591 https://doi.org/10.1016/j.yjmcc.2006.07.006 | PubMed

Hinde E., Cardarelli F., Digman M. A., Gratton E (2010) In vivo pair correlation analysis of EGFP intranuclear diffusion reveals DNA-dependent molecular flow. *Proc Natl Acad Sci U S A* **107**:16560-16565 https://doi.org/10.1073/pnas.1006731107 | PubMed

Hiremath S. V., Goyal E., Reeves G. T., Williams C. M (2024) FRAP analysis: Measuring biophysical kinetic parameters using image analysis. *ArXiv* https://doi.org/10.48550/arXiv.2402.16615

Holzer T., Liffers K., Rahm K., Trageser B., Özbek S., Gradl D (2012) Live imaging of active fluorophore labelled Wnt proteins. *FEBS Letters* **586**:1638-1644 https://doi.org/10.1016/j.febslet.2012.04.035 | PubMed

Isoda K., Nüsslein-Volhard C (1994) Disulfide cross-linking in crude embryonic lysates reveals three complexes of the Drosophila morphogen dorsal and its inhibitor cactus. *Proc Natl Acad Sci U S A* **91**:5350-5354 https://doi.org/10.1073/pnas.91.12.5350 | PubMed

Isoda K., Roth S., Nüsslein-Volhard C (1992) The functional domains of the Drosophila morphogen dorsal: evidence from the analysis of mutants. *Genes Dev* **6**:619-630 https://doi.org/10.1101/gad.6.4.619 | PubMed

Kidd S (1992) Characterization of the Drosophila cactus locus and analysis of interactions between cactus and dorsal proteins. *Cell* **71**:623-635 PubMed | https://doi.org/10.1016/0092-8674(92)90596-5

Liberman L. M., Reeves G. T., Stathopoulos A (2009) Quantitative imaging of the Dorsal nuclear gradient reveals limitations to threshold-dependent patterning in Drosophila. *Proceedings of the National Academy of Sciences of the United States of America* **106**:22317-22322 https://doi.org/10.1073/pnas.0906227106 | PubMed

Lisiero D. N., Cheng Z., Tejera M. M., Neldner B. T., Warrick J. W., Wuerzberger-Davis S. M., Hoffmann A., Suresh M., Miyamoto S (2020) IκBα Nuclear Export Enables 4-1BB–Induced cRel Activation and IL-2 Production to Promote CD8 T Cell Immunity. *The Journal of Immunology* **205**:1540-1553 https://doi.org/10.4049/jimmunol.2000039 | PubMed

Luz M., Spannl-Müller S., Özhan G., Kagermeier-Schenk B., Rhinn M., Weidinger G., Brand M (2014) Dynamic Association with Donor Cell Filopodia and Lipid-Modification Are Essential Features of Wnt8a during Patterning of the Zebrafish Neuroectoderm. *PLoS ONE* **9**:e84922 https://doi.org/10.1371/journal.pone.0084922 | PubMed

Moussian B., Roth S (2005) Dorsoventral axis formation in the Drosophila embryo--shaping and transducing a morphogen gradient. *Curr. Biol* **15**:R887-R899 https://doi.org/10.1016/j.cub.2005.10.026 | PubMed

O'Connell M. D., Reeves G. T (2015) The Presence of Nuclear Cactus in the Early Drosophila Embryo May Extend the Dynamic Range of the Dorsal Gradient. *PLOS Computational Biology* **11**:e1004159 https://doi.org/10.1371/journal.pcbi.1004159 | PubMed

Reach M., Galindo R. L., Towb P., Allen J. L., Karin M., Wasserman S. A (1996) A gradient of cactus protein degradation establishes dorsoventral polarity in the Drosophila embryo. *Dev. Biol* **180**:353-364 https://doi.org/10.1006/dbio.1996.0308 | PubMed

Reeves G. T., Stathopoulos A (2009) Graded dorsal and differential gene regulation in the Drosophila embryo. *Cold Spring Harb Perspect Biol* **1**:a000836 https://doi.org/10.1101/cshperspect.a000836 | PubMed

Reeves G. T., Trisnadi N., Truong T. V, Nahmad M., Katz S., Stathopoulos A (2012) Dorsal-ventral gene expression in the Drosophila embryo reflects the dynamics and precision of the dorsal nuclear gradient. *Developmental Cell* **22**:544-557 https://doi.org/10.1016/j.devcel.2011.12.007 | PubMed

Ribes V., Balaskas N., Sasai N., Cruz C., Dessaud E., Cayuso J., Tozer S., Yang L. L., Novitch B., Marti E., *et al.* (2010) Distinct Sonic Hedgehog signaling dynamics specify floor plate and ventral neuronal progenitors in the vertebrate neural tube. *Genes & Development* **24**:1186-1200 https://doi.org/10.1101/gad.559910 | PubMed

Rippe K (2000) Simultaneous Binding of Two DNA Duplexes to the NtrC−Enhancer Complex Studied by Two-Color Fluorescence Cross-Correlation Spectroscopy. *Biochemistry* **39**:2131-2139 https://doi.org/10.1021/bi9922190 | PubMed

Roth S., Hiromi Y., Godt D., Nüsslein-Volhard C (1991) cactus, a maternal gene required for proper formation of the dorsoventral morphogen gradient in Drosophila embryos. *Development* **112**:371-388 https://doi.org/10.1242/dev.112.2.371 | PubMed

Roth S., Stein D., Nüsslein-Volhard C (1989) A gradient of nuclear localization of the dorsal protein determines dorsoventral pattern in the Drosophila embryo. *Cell* **59**:1189-1202 https://doi.org/10.1016/0092-8674(89)90774-5 | PubMed

Schloop A. E., Bandodkar P. U., Reeves G. T (2020) Formation, interpretation, and regulation of the Drosophila Dorsal/NF-κB gradient. *Current Topics in Developmental Biology* **137**:143-191 https://doi.org/10.1016/bs.ctdb.2019.11.007 | PubMed

Schloop A. E., Carrell-Noel S., Friedman J., Thomas A., Reeves G. T (2020) Mechanism and implications of morphogen shuttling: Lessons learned from dorsal and Cactus in Drosophila. *Developmental Biology* https://doi.org/10.1016/j.ydbio.2020.01.011 | PubMed

Schloop A. E., Hiremath S. V., Shaikh R., Dima S. S., Lizardo L., Bhakta A., Williams C. M., Reeves G. T (2025) Spatiotemporal dynamics of NF-κB/Dorsal inhibitor IκBα/Cactus in Drosophila blastoderm embryos. *IScience* **28**:112854 https://doi.org/10.1016/j.isci.2025.112854 | PubMed

Schneider D. S., Hudson K. L., Lin T. Y., Anderson K. V (1991) Dominant and recessive mutations define functional domains of Toll, a transmembrane protein required for dorsal-ventral polarity in the Drosophila embryo. *Genes & Development* **5**:797-807 https://doi.org/10.1101/gad.5.5.797 | PubMed

Stathopoulos A., Levine M (2002) Dorsal gradient networks in the Drosophila embryo. *Developmental Biology* **246**:57-67 https://doi.org/10.1006/dbio.2002.0652 | PubMed

Stathopoulos A., Levine M. (2004) Whole-genome analysis of Drosophila gastrulation. *Curr. Opin. Genet. Dev* **14**:477-484 https://doi.org/10.1016/j.gde.2004.07.004 | PubMed

Steward R. (1987) Dorsal, an embryonic polarity gene in Drosophila, is homologous to the vertebrate proto-oncogene, c-rel. *Science* **238**:692-694 https://doi.org/10.1126/science.3118464 | PubMed

Steward R., Zusman S. B., Huang L. H., Schedl P (1988) The dorsal protein is distributed in a gradient in early drosophila embryos. *Cell* **55**:487-495 https://doi.org/10.1016/0092-8674(88)90035-9 | PubMed

Teleman A. A., Cohen S. M (2000) Dpp gradient formation in the Drosophila wing imaginal disc. *Cell* **103**:971-980 https://doi.org/10.1016/S0092-8674(00)00199-9 | PubMed

Turpin P., Hay R. T., Dargemont C (1999) Characterization of IκBα Nuclear Import Pathway. *Journal of Biological Chemistry* **274**:6804-6812 https://doi.org/10.1074/jbc.274.10.6804 | PubMed

Wallkamm V., Dörlich R., Rahm K., Klessing T., Nienhaus G. U., Wedlich D., Gradl D (2014) Live Imaging of Xwnt5A-ROR2 Complexes. *PLoS ONE* **9**:e109428 https://doi.org/10.1371/journal.pone.0109428 | PubMed

Wartlick O., Mumcu P., Kicheva A., Bittig T., Seum C., Jülicher F., González-Gaitán M (2011) Dynamics of Dpp signaling and proliferation control. *Science* **331**:1154-1159 https://doi.org/10.1126/science.1200037

Weidemann T., Wachsmuth M., Tewes M., Rippe K., Langowski J (2002) Analysis of Ligand Binding by Two-Colour Fluorescence Cross-Correlation Spectroscopy. *Single Molecules* **3**:49-61 https://doi.org/10.1002/1438-5171(200204)3:1<49::AID-SIMO49>3.0.CO;2-T

Whalen A. M., Steward R (1993) Dissociation of the Dorsal-Cactus complex and phosphorylation of the Dorsal protein correlate with the nuclear localization of Dorsal. *J Cell Biol* **123**:523-534 https://doi.org/10.1083/jcb.123.3.523 | PubMed

Williams P. H., Hagemann A., González-Gaitán M., Smith J. C (2004) Visualizing long-range movement of the morphogen Xnr2 in the Xenopus embryo. *Curr Biol* **14**:1916-1923 https://doi.org/10.1016/j.cub.2004.10.020 | PubMed

Zhou S., Lo W.-C., Suhalim J. L., Digman M. A., Gratton E., Nie Q., Lander A. D (2012) Free Extracellular Diffusion Creates the Dpp Morphogen Gradient of the Drosophila Wing Disc. *Current Biology* **22**:668-675 https://doi.org/10.1016/j.cub.2012.02.065 | PubMed

Peer reviews

Reviewer #1 (Public review):

Summary:

Al Asafen and colleagues here apply a set of scanning fluorescence correlation spectroscopic approaches (Raster Image Correlation Spectroscopy (RICS), cross-correlation RICS, and pair correlation function spectroscopy) to address the nucleo-cytoplasmic kinetics of the Dorsal (Dl) transcription factor in early Drosophila embryos. The Toll/Dl system has long been appreciated to establish dorsal-ventral polarity of the embryo through Toll-dependent control of Dl nuclear localization, and represents one of a handful of model morphogen gradients produced with high enough precision to yield robust biophysical measurements of general transcription factor activity and function. By measurement of GFP-tagged Dl protein, either in wild-type embryos, or in mutant embryos with low/medium/high levels of Toll signaling, the authors report diffusivity of Dl in nuclear and cytoplasmic compartments, as well as the fraction of mobile and immobile Dl, which can be correlated with DNA binding through cross-correlation RICS. A model is presented where Cactus/IkB is implicated in preventing Dl from binding to DNA.

Strengths:

The study uses raster image correlation spectroscopy approaches to measure biophysical components of the Dl gradient in Drosophila embryos. It convincingly demonstrates a positive correlation between Toll pathway activity and the fraction of bound Dl in the nucleus. RICS methodology has widespread potential applications in cell and developmental biology, and this study will contribute to its adoption.

Weaknesses:

The study seeks to test a hypothesis for how the Toll pathway may limit Dl DNA binding in the nucleus. This experiment, while producing initial support for a role of nuclear Cactus, is confounded by co-expression of wild-type Dl, thus limiting the interpretation of the experimental results.

https://doi.org/10.7554/eLife.100462.2.sa2

Reviewer #2 (Public review):

Summary:

In this manuscript, Al Asafen, Clark et al. use fluorescence correlation spectroscopy (FCS) to quantitatively analyze the mobility of Dl along the DV axis of the early Drosophila embryo. Dl is essential for dorsal-ventral (DV) patterning and its gradient initiates the activation of several genes and thereby orchestrates the formation of the Drosophila body plan. While the mechanisms underlying Dl gradient formation have been extensively studied, there are some observations for which there is not yet a mechanistic explanation. For example, the peak of the Dl gradient grows continuously during nuclear cycles 10-14. This is likely due to Cact-dependent Dl diffusion and Dl binding to DNA. But the biophysical parameters governing Dl nuclear dynamics that would support these claims have not been previously measured. In this work, the authors separated GFP-tagged Dl into a mobile and an immobile pools. Interestingly, the fraction of immobile Dl is position-dependent, revealing more binding to DNA in ventral than in dorsal nuclei. This is either due to higher binding affinity in ventral locations (due to Toll-dependent Dl phosphorylation) or to higher Dl-Cact binding in dorsal nuclei that would prevent Dl to bind DNA. Using specific dl alleles, authors support the latter hypothesis.

Strengths:

The manuscript is well written and their conclusions are convincingly supported by their methodology and analysis. As a quantitative study, the biophysical analysis seems rigorous, in general.

Although this is not the first study that employs FSC to investigate the dynamics of a morphogen, it further exemplifies how these quantitative tools can be used to uncover mechanistic aspects of morphogen dynamics during development. In particular, the manuscript reports novel biophysical parameters of Dl dynamics that will be helpful in future hypotheses-driven modeling studies.

Weaknesses:

The main weakness of the manuscript is that the main biological implication of the study, namely that the asymmetry in the fraction of immobile Dl is a result of nuclear Dl-Cact binding which prevents Dl to bind DNA (Figure 5), occurs in a region of the embryo where there is very little Dl anyways (Figure 1A). While it is interesting that a small fraction of immobile Dl significantly increases in dorsal nuclei in mutants expressing a form of Dl with reduced Cact binding it is unclear what is the biological impact of this effect in a location where Dl is nearly absent.

Another weakness of the study, is that experiments are performed in the presence of a wild-type GFP-tagged Dl (unfortunately, the Dl gradient does not form without it; Supplemental Figure 4). This is an unfortunate technical limitation, because it cannot allow to test how important Cact binding is for determining the amount of Dl that could bind DNA in more biologically-relevant locations of the embryo (e.g., in lateral regions).

Overall, I feel that the manuscript exemplify how FSC methods and analysis can be used for the estimation of biophysical parameters and test biological hypothesis, even under very low concentrations (such as Dl in dorsal-most nuclei). However, due to technical limitations, it falls short in offering a real quantitative understanding of their proposed mechanisms. The authors did not report in Figure 5, what happens to the fraction of Dl bound to DNA in lateral regions in the reduced Cact binding and reduced Toll phosphorylation mutants.

https://doi.org/10.7554/eLife.100462.2.sa1

Author response:

The following is the authors' response to the original reviews.

> ***Public Reviews:***
>
> ***Reviewer #1 (Public review):***
>
> *Summary:*
>
> *Al Asafen and colleagues apply a set of scanning fluorescence correlation spectroscopic approaches (Raster Image Correlation Spectroscopy (RICS), cross-correlation RICS, and pair-correlation function spectroscopy) to address the nuclear-cytoplasmic kinetics of the Dorsal (Dl) transcription factor in early Drosophila embryos. The Toll/Dl system has long been appreciated to establish dorsal-ventral polarity of the embryo through Tolldependent control of Dl nuclear localization, and provides an example of a morphogen gradient produced with high enough precision to yield robust biophysical measurements of general transcription factor activity and function. By measuring GFP-tagged Dl protein, either in wild-type embryos or in mutant embryos with low/medium/high levels of Toll signaling, the authors report diffusivity of Dl in nuclear and cytoplasmic compartments of the embryo, as well as the fraction of mobile and immobile Dl, which can be correlated with DNA binding through cross-correlation RICS. A model is presented where Cactus/IkB is implicated in preventing Dl from binding to DNA.*
>
> *Strengths:*
>
> *The experiments on wild-type GFP-tagged Dorsal are performed well, are mostly reported well, and are interpreted fairly.*
>
> *Weaknesses:*
>
> *The discrepancy between experiment and theory as pertains to Michaelis-Menten kinetics is not fully motivated in the text, and could benefit from a more clear presentation. The experiments performed to distinguish between the contribution of Toll-dependent phosphorylation and Cactus interaction models for limiting Dorsal DNA binding are possibly confounded by the presence of wild-type, GFP-tagged Dorsal protein.*

Thank you for your thoughtful feedback. Regarding the discrepancy between experiment and theory in relation to Michaelis-Menten kinetics, we recognize that our initial explanation may not have been explicit enough. Our intent was to illustrate that if DNA binding is a saturable process, then while the absolute concentration of Dl bound to DNA will increase with total Dl levels, the fraction of Dl bound to DNA will decrease. We used Michaelis-Menten kinetics only

as a familiar example to convey this concept but did not intend to suggest that the system strictly follows Michaelis-Menten behavior. To clarify this point, we removed mention of Michaelis-Menten as an illustrative analogy and stuck specifically with discussing the system as "saturating." This primarily affected text in the paragraph starting on Line 204, but also Lines 323-325.

Regarding the concern about potential confounding effects due to the presence of wildtype GFP-tagged Dorsal (Dl[wt]-GFP): we understand the importance of addressing this point more directly. Therefore, we have imaged the Dorsal-GFP gradient in embryos expressing the UAS-dl[S280P]-GFP or the UAS-dl[S317A]-GFP constructs in the absence of the BAC-recombineered Dl-GFP construct. In both cases, the dl mutants by themselves were not able to recapitulate enough of the Dl gradient to test our hypotheses. We have added this analysis to Supplemental Figure 4 and mentioned this figure on Lines 333-336 and 354-358. Furthermore, we explicitly mention that it is possible the reason why we failed to reject the null hypothesis in the Toll phosphorylation mutant case may be due to the additional copy of Dl[wt]-GFP (the BAC recombineered construct), with text added to Lines 343-345, 365-369 (Results) and 408-418 (Discussion).

> ***Reviewer #2 (Public review):***
>
> *Summary:*
>
> *In this manuscript, Al Asafen, Clark et al., use fluorescence correlation spectroscopy (FCS) to quantitatively analyze the mobility of Dl along the DV axis of the early Drosophila embryo. Dl is essential for dorsal-ventral (DV) patterning and its gradient initiates the activation of several genes and thereby orchestrates the formation of the Drosophila body plan. While the mechanisms underlying the formation of the Dl gradient have been extensively studied by this group and others, there are some observations for which there is not yet a mechanistic explanation. For example, the peak of the Dl gradient grows continuously during nuclear cycles 10-14. This is likely due to Cact-dependent Dl diffusion and Dl binding to DNA. However, the biophysical parameters governing Dl nuclear dynamics that would support these claims have not been previously measured. In this work, the authors provide evidence that GFP-tagged Dl may be separated into a mobile pool and an immobile pool. Interestingly, the fraction of immobile Dl is position-dependent along the DV axis, revealing more binding to DNA in the ventral than in the dorsal nuclei. This is either due to higher binding affinity in ventral locations (due to Toll-dependent Dl phosphorylation) or to higher Dl-Cact binding in dorsal nuclei that would prevent Dl from binding to DNA. Using dl-mutant alleles, the authors support the latter hypothesis.*
>
> *Strengths:*
>
> *The manuscript is well written and their conclusions are convincingly supported by their methodology and analysis. As a quantitative study, the biophysical analysis seems rigorous, in general.*
>
> *Although this is not the first study that employs FSC to investigate the dynamics of a morphogen, it further exemplifies how these quantitative tools can be used to uncover mechanistic aspects of morphogen dynamics during development. In particular, the manuscript reports novel biophysical parameters of Dl dynamics that will be helpful in future hypotheses-driven modeling studies.*
>
> *Weaknesses:*
>
> *In my opinion, the main weakness of the manuscript is that the main biological implication of the study, namely that the asymmetry in the fraction of immobile Dl is a result of nuclear Dl-Cact binding which prevents Dl from binding DNA (Figure 5), occurs*

> *in a region of the embryo where there is very little Dl anyways (Figure 1A, 5A). While it is interesting that the fraction of immobile Dl increases (just a little, but significantly) in dorsal nuclei in mutants expressing a form of Dl with reduced Cact binding it is unclear what is the biological impact of this effect in a location where Dl is nearly absent. As can be seen in Figure 3F, the fraction of immobile is unaffected in Dl-mutant forms with reduced DNA binding, because it is already very low. It is unlikely that Dl binding to Cact in dorsal nuclei would affect shuttling as well since the fraction is very low anyway.*

We thank the reviewer for pointing out the places where we could strengthen our explanations. Here we first address the criticism, also raised by the other reviewer, that the fraction of immobile Dl increases only a small amount (Fig. 5A). [In our reply to the next comment, we address the question of biological implications.] We attempted to explain this small effect size in the manuscript; however, we understand that we could clarify further and, given the fact that eLife has no restraints on space, we added more explanation in the main text.

In essence, even though the effect was statistically significant, the effect size was small because the mutation was “diluted” by the presence of a wildtype Dl protein tagged with GFP. We were willing to deal with this dilution because the alternative was that, according to previous literature, without any wildtype Dl, no Dl gradient would be present in the reduced Toll phosphorylation mutants, and only a very weak Dl gradient (weakened on both ends) would be present in mutants that reduced Cact binding. We were confident that, with our quantitative approaches, we would be able to detect the diluted effect.

However, because both reviewers have criticized this diluted effect, in this resubmission, we have included analysis of GFP-tagged mutants without the presence of wildtype Dl protein. Unfortunately, these embryos lack a discernible Dl gradient and cannot be analyzed in such a way as to test the hypotheses that the mutants were generated for.

Even so, the effect of the Cact-binding mutant was strong enough that we were able to statistically distinguish it from embryos expressing only wildtype Dl-GFP, even with the dilution effect. On the other hand we have also included a caveat that our failure to statistically distinguish Toll phosphorylation mutants from wildtype may be due to the dilution effect. We now also explicitly state the concerns about a lack of a discernible Dl gradient and have included figures of full mutants in the supplement. See also our discussion of Reviewer 1’s similar comment.

> *While the authors have a very clear understanding of the biology of the Dl gradient, I feel that the manuscript is more written as a 'tools' paper (i.e., to exemplify how FSC methods and analysis can be used for biological discovery). This is ok, but I think that the authors should discuss further what are the biological implications of these findings other than the contribution to uncovering the biophysical parameters.*

Here we underscore the biological implications of our discovery that Cact is present in the nucleus on the dorsal side. The reviewer mentioned that Cact in the nucleus on the dorsal side appears to have little overall effect, because this is the location of the embryo where there is very little Dl in the first place, which raises the question of whether this discovery is impactful.

While we previously used the final paragraph of the discussion to touch on the implications of this discovery, we acknowledge that we could have spent more time on the explanation. As such, we have expanded this final paragraph into two paragraphs. In the first of the two, we discuss in more detail the implications specifically of the Dl/Cact interactions in the dorsal-most nuclei, as understood by the results of this paper. In brief, knowing that Dl in the dorsal-most nuclei is bound by Cact results in an updated understanding of the Dl gradient, with increased dynamic range, robustness, and precision (but unknown shape).

In the second of the two paragraphs, we discuss this result in light of our recent work on imaging Cact in live embryos, in which we have shown that Cact is present in all nuclei at roughly uniform levels. Taken together, we suggest that it is possible that Cact is bound to Dl in all nuclei (not just the dorsal-most), which would allow us to estimate the shape of the overall Dl gradient by subtracting off the fluorescence that stems from Dl/Cact complex.

> *For example, I think that the implications of the rejected hypothesis (i.e., that Tolldependent Dl phosphorylation does not seem to have an impact on Dl binding affinities to DNA) are important and should be further discussed (even if no additional experiments are performed). What is then the role of Dl phosphorylation? Perhaps it could have an impact on patterning robustness in lateral regions. The authors should report in Figure 5 also what happens to the fraction of Dl bound to DNA in lateral regions in the reduced Cact binding and reduced Toll phosphorylation mutants.*

We appreciate the reviewer's suggestion that the rejection of the hypothesis that phosphorylation of Dl by Toll impacts Dl/DNA binding could be expanded upon further. For the role of Dl phosphorylation by Toll: we previously mentioned that this phosphorylation is known to enhance the nuclear import or retention of Dl, and that mutation of serine 317 to an alanine abolishes Toll-mediated phosphorylation of Dl, which results in embryos with no Dl gradient. We had also mentioned that phosphorylation of Dl is not known to affect its DNA binding, which is the hypothesis we sought to test by creating the dl[S317A]-GFP mutants. We did not image any mutants, or the UAS-dl[wt]-GFP control, in the lateral regions, for two reasons. First, this region is easily the smallest of the three regions, in terms of the percentage of the DV axis (see Fig. 1A). Second, because of the dilution effect, we knew the effect size would be small, and as such, we imaged only on the extreme ends of the gradient so that the most clear conclusion could be drawn about the effect that Toll phosphorylation might have on DNA binding of Dl.

> *The way that position along the DV axis is reported using the nuclear-cytoplasmic-ratio (NCR) in Figures 1-3 is not incorrect, but I wonder if it is the best way of doing it. The reason is that it spreads out a relatively small region of the embryo (the ventral-most locations) and shrinks a relatively large region of the embryo (lateral and dorsal regions), see Figure 1A. Perhaps reporting the NCR in log_2 units would be more appropriate.*

We agree that there is some distortion of the relative spatial extents of the Dorsal gradient when NCR is used as an independent variable on a plot. However, we prefer the NCR on the horizontal axis because it is closer the functional variable (Dl concentration, rather than spatial location) for the properties we studied.

> ***Recommendations for the authors:***
>
> ***Reviewer #1 (Recommendations for the authors):***
>
> *I really enjoyed the first part of this paper and have only minor suggestions for improvement of the presentation. I am confused about the experimental approach for the final figure, distinguishing phosphorylation and cactus-dependent effects. I'll divide my comments between "First Part/General Suggestions", "Last Part", and finish with some minor typo observations.*
>
> *The gist of the issues with the last part of the paper could boil down to insufficient detail/explanation of the section. The discrepancy with expectation with Michaelis-Menten kinetics is presented in a total of three sentences and is not necessarily obvious to the general readership of eLife. The mutants chosen to distinguish the phosphorylation and cactus mechanisms could be described more (why these? aren't other residues phosphorylated?) and possibly why also having wild-type GFP-Dl in the*

> *measurements isn't confounding. Since there is unlimited space in this journal, it may be advisable to use this space to fill out these rationales and ideas.*
>
> *First part/General Suggestions:*
>
> *(1) For the RICS data, (Figures 1 and 2) there is a nice correlation between WT NC ratio and the selected low/med/hi Dl activity mutants. More-or-less the median values in, say, Figure 1E-G are reflected in Figure 1H. However, with the ccRICS data (Figure 3), it looks like there is less correspondence between the range of fraction bound estimates in, for instance, "ventral" in Figure 3D and '10b' in Figure 3E. Can the authors comment on this? Should the reader be able to make this kind of comparison, or does something about data collection for the wt/NCR measurements preclude direct comparison of magnitudes with the panel of mutants? (imaging setup, laser power, etc)?*

The reviewer is correct that there seems to be a discrepancy in the values of ψ between the wt embryos (ventral side) and the Toll10B embryos. It should be noted that the Toll10B embryos are not “ventral-like” in every way, in part because they have unknown activated Toll levels that might be above or below what is seen at the ventral midline in wildtype embryos, and in part because there is no DV gradient, and thus no shuttling in these embryos that would accumulate total Dorsal on the ventral midline. As such, comparisons between Toll10B embryos and the ventral side of wildtype embryos are not exactly one-toone, and we are more confident in comparing among the mutants in an allelic series. To address this question, we have added a sentence to the end of the second paragraph of the “Dorsal/DNA binding exhibits a spatial gradient” subsection of the Results (Lines 233235).

> *(2) Materials and methods: Mounting and imaging of Drosophila embryos: the authors cite the "488 nm laser intensity ranged from 0.5% to 3.0%..." The values presented here are not useful for the general reader or an individual looking to replicate these conditions, as emission power produced from such values will vary from instrument to instrument. It is standard in these cases to report an estimated laser power (measured in watts) for each laser line, and a clear description of how such measurements were made (stationary beam, under scanning conditions, with what detector, etc). These measurements are valuable and the authors are strongly encouraged to report such measurements for their setup.*

We appreciate the reviewer’s suggestion and understand the importance of providing absolute laser power values for reproducibility. We have now included the laser power (in watts) for the laser lines on both microscopes used in this study. The revised text can be found in the Materials and Methods section, in the Lines 535-536 and 540.

> *(3) The presentation of the data in Figure 4 is difficult to understand. Are the kymographs (A lower) representing the entire length of the big white arrow in A upper? Or do the dashed lines indicate the x-axis limits of the kymograph? It is difficult to tell from the figure legend, where the dashed lines are described as "areas where Dl-GFP movement is measured out of the nucleus." I believe that the authors can make these measurements and that Figure 4B reflects properties of "movement" of Dl out of the nucleus, but how they get there from these data is not clear to this reader. Perhaps a cartoon explaining the green lines and the orange lines in the kymograph or tightening the legend would help.*

We thank the reviewer for their feedback and understand the need for greater clarity in the text of the pCF section and in Figure 4. The widths of the kymographs in the lower panels correspond to the full widths of the images in the upper panels. The pCF measurements were taken at the y-coordinates at the level of the white arrows. The dashed vertical lines connecting the upper and lower panels illustrate two cases of locations along the x-axis of the image where Dl is crossing from inside a nucleus to outside. In the two illustrated cases, these

crossings are accompanied by either zero Dl molecules being observed to cross the nuclear barrier (ventral image/kymograph on left) or delayed crossing of Dl molecules (dorsal image/kymograph on right). To address this concern, we have added more detail to the Fig. 4 legend and greatly expanded on a discussion of what pCF does in the text (the second and third paragraph of the section). We have also updated Fig. 4 to align with new explanations from the text: namely, describing the y-axis of the kymographs as Δt (instead of log(time)) and explicitly showing that the pair correlation is for pairs of pixels that are Δx = 6 pixels apart. Further details were also added to the relevant Methods section.

> *(4) DV position in the wild-type imaging experiments is operationally determined through measurement of the Dorsal NC ratio. This makes sense, but the strategy is buried in the first paragraph of the results, and not discussed in the M & M. For readers unfamiliar with imaging the fly embryo or the nuances of the Dl gradient, perhaps a sentence or two explaining that embryos were oriented randomly along the DV axis, and DV positions of the imaging region were estimated by measuring the Dl NC ratio.*

We thank the reviewer for this helpful suggestion. To improve clarity, we have added a description of how DV position was determined to the Materials & Methods section (paragraph starting on Line 520). Specifically, we now state that embryos were randomly oriented along the DV axis and that we used the Dorsal NC ratio of intensity as a proxy for measuring the DV position in imaging experiments. Additionally, we have added a statement to the Results section to ensure that this strategy is more clearly introduced (Lines 143-144). We appreciate this recommendation, as it will help readers unfamiliar with fly embryo imaging better understand our approach.

> *(5) It would be nice to report the corresponding NC-ratio values for Dl in each of the mutant conditions, perhaps as a supplement to Figure 1. Currently, Figure 1H relies on the (admittedly well-established) properties of the three mutants, but it feels that an additional nice quantitative link in the data can be drawn out here. Do the authors see the strict correlation between the wt and mutant diffusivity measurements at specific NC-ratios?*

We are hesitant to try to draw direct comparisons between the mutants and the behavior of the wildtype embryo at the corresponding NCR. This is because, in the context of these uniform mutants, the NCR is determined by a combination of at least three factors that we cannot measure or control for: the unknown strength of Toll signaling, the unknown capacity of Toll signaling (ie, the potential saturation of the cytoplasmic enzymes controlled by Toll signaling), and, most importantly, the lack of a shuttling mechanism that concentrates Dl on the ventral side of the embryo. As such, the NCR does not represent a continuous variable that transforms the behavior of one mutant into another (or from mutants into wt DV coordinates), as it does along the DV axis in wildtype embryo. This is why the mutant studies are presented as boxplots. At best, we were comfortable only in using the uniform mutants as an allelic series to produce gross trends. We have added a brief statement describing the shuttling caveat to the Results section (Lines 173-177).

> *(6) In the section related to Dl nuclear export, the language used to describe Dl kinetics is ambiguous. The term "movement" is used seemingly as a catch-all for nuclear-importexport as distinguished from diffusion. However, diffusion is also a form of movement. Could this section be reworked to explicitly distinguish nuclear import-export and diffusive movements?*

We appreciate the reviewer's suggestion and agree that the language used to describe Dl kinetics could be more precise. By way of explanation, the pCF analysis calculates the time scale on which Dl can exit the nucleus. pCF only gives a signal if it sees the same Dl molecule twice, at two different locations after some Δt amount of time has passed. Because of this, if a given Dl molecule in a ventral nucleus is being tracked, then that molecule has some

probability that it is bound to DNA initially, which means it will take, on average, longer to exit the nucleus than a Dl molecule not initially bound to DNA. Therefore, on the ventral side, the time scale on which Dl exits the nucleus is longer than on the dorsal side (where DNA binding is not happening). This can be true even if the nuclear export rate constants are the same on the ventral side vs the dorsal side. As such, we were careful to choose language that did not imply that we were talking about a nuclear export rate constant. We have added this discussion to the end of the relevant Results section (Lines 308-315).

We have also revised this section to explicitly distinguish between the mobility associated with exiting the nucleus and diffusive movement, while still trying to distinguish between the time scale of exiting the nucleus vs the nuclear export rate. Specifically, we now refer to 'time scale of nuclear export' when discussing transport across the nuclear envelope and reserve the term 'diffusion' for passive intracellular movement. Furthermore, we have edited a sentence in this section (Lines 291-293) to describe the distinction we are making between the time scale measured by pCF and the time scale commonly associated with nuclear export (that is, the reciprocal of the rate constant). We hope this clarification improves readability and conceptual clarity.

> *Last Part:*
>
> *(1) There is an undersold argument centered on Michaelis-Menten kinetics that needs to be explicitly presented, especially since it motivates the final experiments of the paper, which are challenging. In the two sections describing how the data do not adhere to expectations based on Michaelis-Menten Kinetics, the assertion that "the fraction of immoble Dl is expected to decrease with increasing nuclear total Dl concentration" is only intuitively true if the system is saturated. Is the system demonstrably saturated? Another interpretation of this would be that these results demonstrate that the system is likely not saturated. In any case, the authors need to devote some space in the introduction and/or results and/or discussion to fully motivate this point.*

We agree that the reviewer has raised an important point: if the system is very far from saturation, then the fraction of immobile Dl is not expected to decrease with increasing nuclear total Dl concentration. But neither would it increase; it would instead stay flat. To correct this mistake, we have edited the sentences in question to acknowledge the farfrom-saturation scenario, saying "at best, [the fraction bound] remain[s] constant" (Line 209). As such, our original point, which is that in no case would the fraction immobile increase [unless something else is going on besides affinity-based binding to DNA], it still valid.

> *(2) Wouldn't any argument on the basis of Michaelis-Menten need to rely on the assumption that the system is at steady-state? Reeves 2012 concludes that during the times measured here, Dl does not reach a steady state. It would be good, in the context of the point above, for the authors to clarify how this impacts the expectations of saturation and the application of M/M kinetics.*

We thank the reviewer for raising this important point. We apologize for not being clear on our points about M/M kinetics and would like to stress again that we are not claiming the system is has M/M kinetics. We appealed to M/M kinetics only as a simple, intuitive example of a saturating system to point out the difference between bound concentration vs bound fraction as functions of total concentration. We did this because previous feedback on our manuscript suggested that the difference between these two variables needed to be made clearer. Because this point seemed controversial with both reviewers, we removed all mention of M/M kinetics and simply refer to the system as "saturating." For further explanation, see the first paragraph of our response to Reviewer 1's "weaknesses" in the public review.

> *(3) It is not clear to me how the inclusion of wild-type, GFP-tagged dorsal in the experimental setup for Figure 5 is not confounding. For the S317 (phospho-) mutant, GFPtagged alleles of both phospho- and wild-type Dl are expressed. The reasoning is that not enough phospho-mutant Dl gets into the nucleus, and this makes it difficult to distinguish the dorsal from the ventral side of the embryo, so in a dl mutant background, there is expression of wt GFP-dl from a BAC, and nos>Gal4 driven expression of a GFP-tagged S317A mutant dl. The measurements show that on the ventral side of the embryo, there is no difference in the fraction of bound Dl. Couldn't this be predominantly binding of wildtype GFP-Dl? How is this interpretable? Wouldn't it be easier to perform these measurements in a Tl 10b background (or to cross in UAS>Tl[10b]) and for the only GFPtagged dl to be S317A? The same goes for the S234 mutant (could be done in the pelle mutant background).*

We thank the reviewer for raising the point that the confounding effect of wildtype Dl makes it difficult to interpret the results from the 317A mutant. Under the circumstances of the experimental design, we can best conclude that, if the null hypothesis is incorrect, the effect size was too small to detect with our sample size. As such, we have modified our discussion of the results of this experiment to carefully explain this caveat (rather than confidently saying that Toll phosphorylation has no effect). For further explanation, see the second paragraph of our response to Reviewer 1's "weaknesses" in the public review, as well as our response to the related question raised by Reviewer 2 in the public review.

> *Minor issues/typo stuff:*
>
> *(1) This reviewer notes that the submitted materials contain neither line numbers nor page numbers.*

We appreciate the reviewer's feedback. We have now included line numbers and page numbers in the revised manuscript for easier reference.

> *(2) First paragraph of results: "We imaged small regions of the embryo..." The parenthetical statement only cites pixel size and directs the reader to the methods. Without the total number of pixels, the pixel size value does not clarify how "small" the imaged region is. Consider including the xy area, pixel dimensions, and pixel size here to assert the smallness of the imaged area.*

We have added the requested information.

> *(3) Second paragraph, Introduction: "Dorsal, one of three (Drosophila) homologs to mammalian NF-kB" (Add Drosophila). Also, aren't these orthologs?*

We have made these changes.

> *(4) Last sentence of last paragraph in the introduction: Kind of a throw-away sentence. Consider revising.*

We thank the reviewer for making this point; the sentence was originally constructed to state that our quantitative measurements resulted in a biologically significant discovery. However, because Reviewer 2 also mentioned the question of biological significance, we have changed this final sentence to explicitly mention of what the biological significance is: namely, an understanding of the Dl gradient that has superior dynamic range, spatial range, robustness, and precision.

> *(5) Where is the median line in the S317A boxplot in Fig 5C?*

The median line is at $\psi = 0$. We have added an explanation of this to the Figure legend.

> *(6) Materials & Methods: Fly transformation, typo: Drosophila embryos were injected with 0.5 µl of each pUAST construct..." The volume of an entire Drosophila embryo is less than 0.5 µl, please revise the units to reflect the value injected. Most likely an absolute volume unit was stated when rather a concentration of an injection solution, delivered at significantly smaller volumes was intended.*

We thank the reviewer for catching this typo. It was intended to indicate a concentration of 0.5 ng/µL, and we have made the appropriate changes.

> ***Reviewer #2 (Recommendations for the authors):***
>
> *(1) Perhaps this has been described in a prior publication (if this is the case, please simply state this somewhere in the Methods section where Dl-GFP embryos are described), but since Dl-GFP embryos have one copy of endogenous dl and one copy of Dl-GFP, how do potential differences in tagged vs. non-tagged Dl interactions with DNA or Cact affect their findings?*

The reviewer brings up a good point, and we acknowledge that any time a protein is tagged with GFP, the behavior of the protein may be affected. We have now explicitly added this caveat to our discussion in a new paragraph on Lines 420-429.

> *(2) In the Discussion section, the authors argue that a major implication of their findings is the possibility that Cact binds Dl in the nuclei would imply that the true (active) Dl gradient may be unknown unless the unbounded Dl is separated from the Dl/Cact (inactive form). While this is an interesting point, this idea is not supported by the findings of Figure 5B where there is no effect in the fraction of Dl bound to DNA in the reduced Cactus binding mutants. The authors should report what happens in lateral regions in Figure 5 because perhaps there is an effect there (see comment on this in the Public Review).*

We thank the reviewer for the insight, as we did not directly discuss the implications of the middle column of Fig. 5B on our hypothesis. Indeed, our hypothesis is not supported by Fig. 5B; it is instead inconclusive (failure to reject H0). This is why we designed the second experiment (Fig. 5C) to test the Cactus hypothesis, because the effect size would be greater on the dorsal side.

Furthermore, as pointed out by both reviewers, the presence of wildtype Dl-GFP in these experiments is confounding. We have discussed this elsewhere in our rebuttal, but briefly, this problem resulted in needing larger effect sizes to detect a statistically significant difference between wt and the mutant populations. This was a necessary evil that we were willing to deal with in order to ensure the Dl gradient could be established so that the dorsal vs ventral sides would be distinguishable. We have added a fuller discussion of these issues to the relevant Results section (Lines 333-336, 343-345, 354-359, 365-369) and also the Discussion section (Lines 412-418), including underscoring the fact that, from a falsification standpoint, the results in Fig. 5B do not allow us to reject either null hypothesis, possibly due to the confounding effect of wildtype Dl. We appreciate the reviewer's point about this, and believe the changes suggested by the reviewer have improved the manuscript.

On the other hand, we respectfully disagree with the reviewer that investigating either mutant in the lateral regions of the embryo would bear fruit. To the first approximation, it would be the average between the behaviors on the ventral vs. dorsal sides. For the S317A mutant, neither the ventral nor the dorsal side was conclusive in regards to our hypotheses. (Although we admit here that further investigation into why the S317A column in Fig. 5C was statistically different from wildtype, in the opposite direction from the S234P mutant, may be interesting in future work.) For the S234P mutant, the data were more conclusive on the side of the embryo where the effect size was expected to be large enough to detect a difference. In

the lateral regions, the expectation would be that the effect size would be intermediate, which would make the interpretation of the results more difficult (i.e., more likely to be inconclusive). In contrast, as Fig. 5C is already conclusive, we are not confident there would be more information gained by imaging the lateral regions.

> *(3) Is Figure 5A a wild-type embryo? If so, I think that the labels are misleading or unclear. Also, is it the same image as in Figure 1A? If so, I suggest replacing this with a schematic since it does not add any new data.*

We have eliminated the labels for the mutants and have added the following comment to the figure 5 legend “Same embryo as in Fig. 1A”.

> *(4) Also in Figure 5, I suggest using labels to indicate the schematics instead of simply using their location. You could use 5A', 5A'' and 5A''', for example.*

We have made the suggested changes.

> *(5) The use of some technical labels makes some figures difficult to read. I suggest using more simple labels for mutants in Figure 3F (replace R063C) or Figure 5B, C (replace S234P and S317A).*

We have made changes to Fig. 3F, Fig. 5B,C, and the corresponding places in the figure legends. We have labeled R063C as ↓DNA, S317A as ↓Toll, and S234P as ↓Cact.

> *(6) I suggest reporting p-values consistently. For example, in Figure 4B, they use one or two asterisks to denote p-values less than 0.07 and 0.05, respectively, which is somehow arbitrary and unconventional. Why not report the actual values as in Figure 5C, for example? (By the way, I would report in Figure 5B the actual p-values as well, since a nonsignificant value is also reported in Figure 5C. Also in Figure 5C, report values in the same notation (decimal or scientific), i.e., either put 0.005 as 5x10^-3 or 10^-3 as 0.001).*

We have made the suggested changes.

https://doi.org/10.7554/eLife.100462.2.sa0